corewind

D1.6
Design Recommendations and Impact of Mooring and Dynamic Cables Into Integrated Modelling and Structural Design

UPC / RAMBOLL / DTU / COBRA / FIHAC / INNOSEA / JDR

March 2023

Disclaimer:

This project has received funding from the European Union's Horizon 2020 Research and Innovation programme under grant agreement No 815083.

Project details:

Duration:
1 Sep 2019 - 28 Feb 2023
Grant agreement:
No: 815083

Document information

Deliverable number	D1.6
Deliverable name	Design Recommendations and Impact of Mooring and Dynamic Cables Into Integrated Modelling and Structural Design
Reviewed by	Sithik Aliyar(DTU), Jannis Espelage (RAMBOLL)
Date	31.03.2023
Work Package and Task	WP1, Task 1.5
Lead Beneficiary for this Deliverable	RAMBOLL
Dissemination level	Public

Authors

Name	Organisation
Pau Trubat, Climent Molins, Daniel Alarcon	UPC
Friedemann Borisade	RAMBOLL
Ozan Gözcü , Henrik Bredmose	DTU
Ignacio Romero	COBRA
Diego Sisí	ESTEYCO
Raúl Guanche, Miguel Somoano	FIHAC
Maxime Chemineau	INNOSEA
Siobhan Doole	JDR

Version control

Version	Date	Author	Description of Changes
1	14/02/2023		First draft
2	31/03/2023		Final

Table of Content

1 Nomenclature

Abbreviation	Description
ALS	Accidental Limit State
DLC	Design Load Case
DOF	Degree of Freedom
EC2	EuroCode 2
FEM	Finite Element Model
FLS	Fatigue Limit State
FOWT	Floating Offshore Wind Turbine
LC	Load Case
LCOE	Levelized Cost Of Electricity
MSL	Mean Sea Level
PLRS	Peak Load Reduction System
ULS	Ultimate Limit State

2 Executive Summary

The purpose of this report is to present COREWIND results related to mooring and cable design and its influence on FOWT response as well as design recommendations from the structural point of view. Results from station keeping predesign, mooring optimized designs, cable influence and experimental results are used to perform an overview analysis of the mooring and cable influence. Design recommendations are given from a structural point of view. First, a standard review for structural design is performed. Second, the main design bases followed for the design are presented, and, third, some detailed examples for the designs are given, for the whole platform, as well as for particular zones like the mooring connection points.

The results comparison is performed for the available data generated during the project. Most of this data was generated for a specific objective, so then, a cross comparison for all the data is difficult to perform due to the differences on DLC conditions and outputs. However, a general trend of the influence of the mooring system and the cable designs can be extracted. The main variables studied are the platform motions (Surge, Sway, Heave, Roll, Pitch and Yaw), Nacelle accelerations (Ax, Ay and Az), tower base bending moments (TwrBsMxt, TwrBsMyt, TwrBsMzt) and fairlead tensions (FairTenXX). The sites analysed are Gran Canaria and Morro Bay for both platforms, ActiveFloat and WindCrete. West of Barra was excluded for WindCrete as non-feasible design, due to the lack of depth for this type of substructure. Also, West of Barra was excluded for Active Float results comparison, as the final optimized mooring design is very different from the predesign one, with an important increase of the number of mooring lines, due to the location presents a very harsh environment. Moreover, it has to be noted, that the optimized mooring system designs for all sites and platforms fulfil ULS but FLS are not verified. On the other hand, the experimental results are performed with a truncated mooring system based on the optimized mooring system from Gran Canaria site. The Table 2-1 and Table 2-2 show a summary of the data comparison for WindCrete and Active Float respectively for Gran Canaria site and DLC 1.6. The results show good agreement between models. For WindCrete, the optimized mooring system shows similar trends between models. The platform motion presents larger pitch for the optimized mooring system due to the large number of LC analysed. However, the optimized mooring system presents a reduction of the nacelle accelerations and a slight increase of the fairlead tensions. For Active Float, the optimized mooring system induces a more compliant platform with larger motions in surge and larger Yaw rotations. In this case the accelerations at the nacelle are increased, but the line tensions are reduced at the fairleads.

Table 2-1: WindCrete DLC1.6 comparison for the Predesign, Optimized and Experimental mooring systems

WindCrete	Surge [m]	Sway [m]	Heave [m]	Roll [deg]	Pitch [deg]	Yaw [deg]
Predesign	13.2	5.1	1.5	3.0	5.5	8.3
Optimized	12.5	9.7	1.4	6.8	7.4	8.6
Experimental	12.34	10.68	3.07	1.64	6.34	1.63
	Ax [m/s²]	**Ay [m/s²]**	**Az [m/s²]**			
Predesign	2.10	0.56	0.43			
Optimized	1.1	0.85	0.34			
Experimental	1.74	0.7	0.14			
	FairTen11[N]	**FairTen12[N]**	**FairTen21[N]**	**FairTen22[N]**	**FairTen31[N]**	**FairTen32[N]**
Predesign	4.39E+06	4.48E+06	2.88E+06	3.85E+06	3.82E+06	2.86E+06
Optimized	3.70E+06	5.07E+06	2.64E+06	3.45E+06	2.59E+06	3.11E+06
Experimental	4.39E+06	3.79E+06	2.71E+06	2.96E+06	3.17E+06	3.23E+06

Table 2-2: ActiveFloat DLC1.6 comparison for the Predesign, Optimized and Experimental mooring systems

ActiveFloat	Surge [m]	Sway [m]	Heave [m]	Roll [deg]	Pitch [deg]	Yaw [deg]
Predesign	20.4	3.0	0.9	2.6	4.0	11.7
Optimized	50.9	32	0.4	5	4.7	28.6
Experimental	46.94	21.97	1.84	1.28	5.43	9.87
	Ax [m/s^2]	**Ay [m/s^2]**	**Az [m/s^2]**			
Predesign	1.5	0.8	0.6			
Optimized	2	1	0.7			
Experimental	0.93	0.5	0.58			
	FairTen1[N]	**FairTen2[N]**	**FairTen3[N]**			
Predesign	6.23E+06	2.97E+06	3.08E+06			
Optimized	4.99E+06	6.94E+05	5.71E+05			
Experimental	5.30E+06	5.85E+05	4.54E+05			

The comparison of the simulations do not give specific trends for both platforms and mooring system models. However, some general trends can arise from the comparison. The differences between mooring systems rely on the behaviour of the predesign mooring system. However, the optimization process leads to more stable solutions and lower mooring tension, with a general trend of nacelle accelerations reductions, which the mooring system also benefits from. The optimization process followed in the optimized mooring system and in the Peak Load Reduction System (PLRS) designs achieved mooring designs that fulfil ULS in both cases. For the optimized mooring system, significant cost reductions were achieved. However, for the PLRS, the increase of costs due to the new equipment does not benefit for the reduction of line tensions. The motions of the platform for the optimized ones have no common trend between WindCrete and ActiveFloat. WindCrete optimized mooring designs tend to reduce platform motions, whereas ActiveFloat ones implies a more compliant structure within the motion DOFs. Then, optimized mooring system differences rely on the initial behaviour of mooring system predesigns

Results from dynamic cable modelling and testing shows the cable system loading on the platform has a negligible influence on moored platform motion. Cable system loading and exit angle requirements based on the cable system designed should be taken into account during the structural design of the cable entrance to platform. Design drivers for the cable system (such as reduction in costing) can impact the loading on this part for the structure on the platform, so a balance between structural design and cable system design is needed. In addition, care should be taken in platform's cable routing structure design to facilitate the smooth disconnection of the cabling system (for planned disconnection cases for maintenance of the platform, and for emergency disconnections) to prevent damage to the structure and minimise damage to the dynamic cabling. Unlike static windfarms (where cable systems are generally designed to fit in with predefined static turbine support structures), due to the inter-dependencies of the moored floating wind structure and the cabling system, the allowable motion for the moored platform structure needs to be considered with limits and cost impact on the cable system design, particularly in regards to target platform excursions relative to water depth.

The mooring connection can be design by a steel plate where the fairlead is welded, and the plate is attached to the concrete wall by means of posttensioning bars. Also, shear lugs or headed struts can be used to improve shear strength. The posttensioning bars are designed in order to balance the mooring line tension loads while allowing for a compression surplus to provide shear strength by means of friction forces. The fairlead is composed

of two vertical and two horizontal padeyes where shafts are installed allowing the fairlead to rotate in vertical and horizontal directions. The Figure 2-1 shows a sketch of the mooring connection with the described elements, for Active Float (left) and WindCrete (right) platforms. It can be seen, that the WindCrete one is equipped with two vertical shafts to allow the installation of two different delta lines. Moreover, in both designs, no posttensioning bars are placed within the vertical and horizontal padeyes to allow place for the shafts.

The design basis followed to obtain the design are the followings:

- Design loads should be based on the capacity of the mooring or alternatively assessed based on the design loads obtained by the hydrodynamic simulations, including the ALS conditions.
- Anchor bolts and their post-tensioned forces should be designed so that there is no decompression under the base plate for the characteristic extreme load combination to avoid fatigue at the posttensioning bars.
- The ultimate capacity of the anchor bolts shall be verified under the ULS and the ALS combinations allowing for plate decompressions. Special care into the tension increase in the post-tensioning bars have to be revised when decompressions occurs, as well as the shear friction reduction.
- A final fatigue assessment of the anchor bolts, reinforcement and concrete shall be carried out. In this, the beneficial effect of posttensioning is remarkable, as it significantly reduces the stress range of the bars and on the contact.
- Watertight and cracking limits of the concrete shall be controlled.

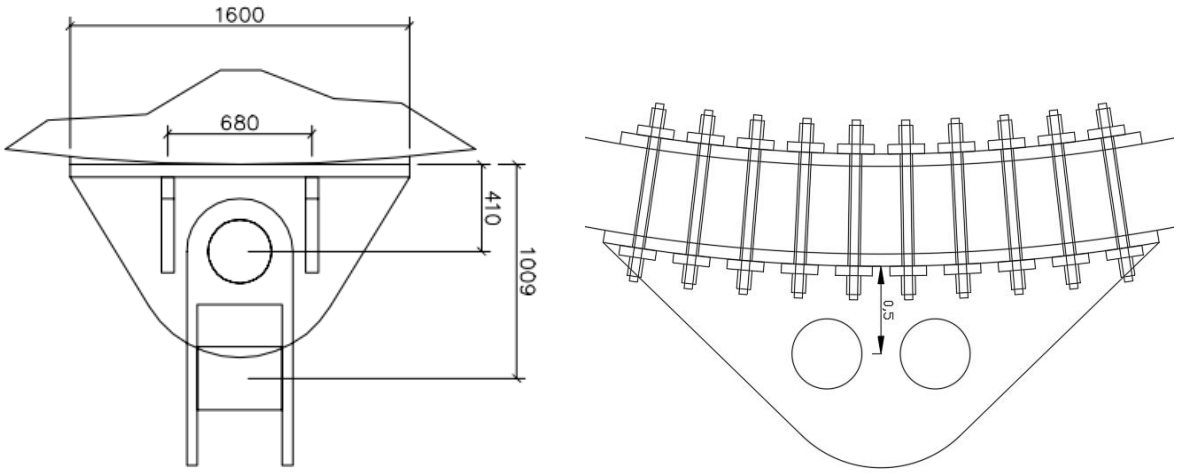

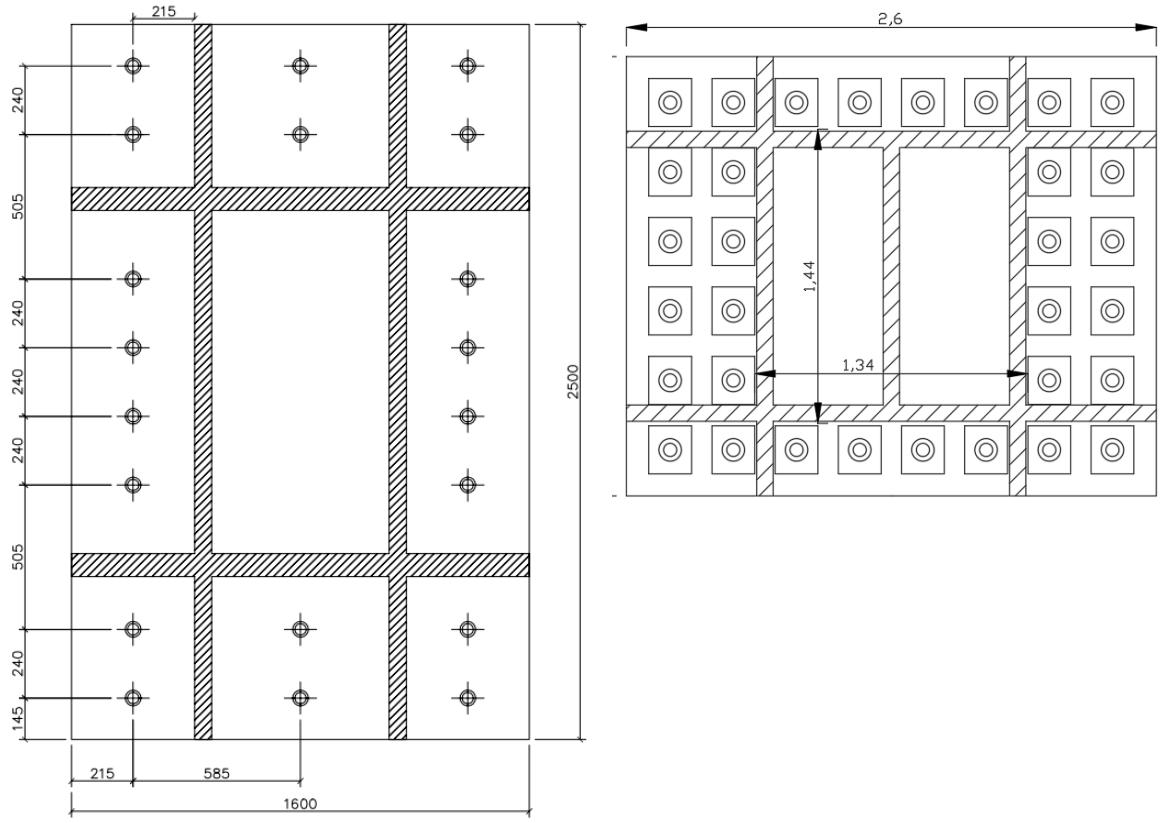

Figure 2-1: ActiveFloat(left in mm) and WindCrete (right in m) mooring connection designs

The structural design of the platform is based on the interrelation of different aspects: main platform dimensions that provide the hydrostatic and physical properties, the concrete properties, the external loads from the wind turbine aerodynamics and the hydrodynamics. The design process aims to reduce costs of the platform while keeping a proper performance within the operational and design limits and ensuring a feasible structural design.

The main aspects that effect on the structural design are the following:

- Life span and exposure class: Exposure classes are one of the main constraints to define the concrete characteristics, and jointly with the life span of the platform are the main drivers to determine the concrete cover.
- Concrete strength: The concrete strength is defined based on the needed section strength to balance the external loads. Moreover, mean concrete stress to concrete strength ratio is related to fatigue in concrete sections.
- DLC 16 and DLC 62 are found to be the main driven DLC for the platform design
- Active reinforcement design is limited by the maximum compressions stress allowed at the concrete sections, but on the other hand, have to guarantee the water-tightness stress limitations for requested sections.
- Water-tightness is a strong factor related to concrete design. Sections that can influence on the damage stability of the platform shall be designed with minimum compressive stress of 0.5MPa. Then, special considerations have to be applied to ensure such stress state.
- Construction and installation process may be driven structural design cases for certain section of the structure

- Finite elements analysis models as well as detailed section analysis are required for a proper structural design analysis.
- Local strengthening of the cylindrical walls of the two floaters is required in the sections where fairleads are connected because the forces on the fairleads are above 5 MN.
- Both floaters do not present connections. They are monolithic substructures.

3 Introduction

The COREWIND project aims to achieve LCOE reduction by means of mooring and cable optimization. The new station keeping systems can have an impact from the structural point of view due to the change of mooring tensions and differences in translational and yaw stiffness. These impacts can influence the final structural design as well as the operational limits of the FOWTs.

COREWIND FOWT designs, WindCrete and ActiveFloat, were designed and presented in D1.3 [1]. These designs were developed using a pre-design mooring system that was not optimized. Then, D2.2 [2] presented a comprehensive optimization study for the station keeping systems of both platforms for all the proposed sites, West of Barra, Morro Bay and Gran Canaria. However, it has to be noted, that the optimized designs fulfil ULS design bases, but FLS design criteria was not fulfilled. From the optimized mooring system designs, D2.3 [3] explored the possibilities of using Peak Tension reduction systems which showed promising results, but cost increases do not compensate the tension reduction on the line. In the D5.3 [4], a detailed report of the experimental test results performed in FIHAC for each platform with platform operational and design limits as well as mooring line tensions is presented. From the structural design point of view, D2.2 presents a design methodology and the final design of the mooring connection to the structure, based on steel plates attached by means of post-tensioning bars.

This deliverable D1.6 is focused on the task 1.5 results and provides a detailed review and comparison of the simulated data and the experimental results performed during COREWIND projects. The aim of the result comparison is to assess the influence of the optimized mooring systems and the dynamic cable on the FOWT operational and design limits from the structural design point of view. Section 4 shows the result comparison of the mooring analysis. The results presented are: 1) the comparison between the pre-design and optimized mooring systems, 2) the comparison between the optimized mooring system and two different peak tension reduction systems, and 3) the results of the experimental tests. In section 5, based on the dyinamic cable modelling and system requirements, the cable influence on the structural design of the platform is reviewed, discussing both structural loading and functional design aspects.

The impacts on the structural design are presented in Section 6 and 7. In section 6 design recommendations for the design of the mooring connections to the anchors are presented, focusing on the design basis and the description of a feasible solution based on a steel plate anchored to the concrete wall through post-tensioning bars. In section 7, design recommendations for the design of the whole structure are given. First, an overview of applicable main standards is presented, and second the influence of main design parameters is shown. Finally, some detailed examples of design particularities for each platform are shown. At the end of this report, conclusions are presented.

4 Mooring Design Optimisation and Implications on Load Assessment

The objective of this section is to analyse and compare the differences between the response obtained by the optimized mooring system and the non-optimized ones, coming from the pre-design in D2.2 of the WindCrete and ActiveFloat platforms. The analysis is performed using OpenFast software package and the comparison is made in terms of mooring tensions, but also in terms of platform operational limits (accelerations, platform motions) and tower loads. Also, the influence of the peak load reduction system (D2.3) on the mooring system is presented.

4.1 Analysis and comparison between predesign mooring systems and optimized ones

The results compared for each mooring design have to be treated in general trends because the compared results come from very different DLC setups. The pre-design setups are based on D1.3, where the platform and the mooring system were analysed for a reduced number of LCs. For the DLC1.6 five simulations with different wind speed were analysed (8, 10.5, 16, 20 and 25 m/s) without wind misalignment. For the DLC6.1 one simulation was performed. On the other hand, for the optimized mooring systems, the DLC simulations were performed using different wind seeds, accounting for wind misalignment and tides which lead to 215 simulations for DLC1.6 and 36 simulations for DLC6.1. Then, it is important to notice that optimized designs have been analysed for a larger number of LCs which can lead to larger load combinations.

4.1.1 WindCrete mooring system designs

The WindCrete design results analysed in this section are the Gran Canaria site and the Morro Bay site. More details about the designs can be found in D1.3 and D2.2. The Figure 4-1 and Figure 4-2 show a sketch of the WindCrete mooring line configuration for Gran Canaria and Morro Bay site with the nomenclature of the tension for each delta line and its view on the simulations. In Morro Bay case, the mooring line configuration is set with 4 main delta line, 90 degrees equally spaced.

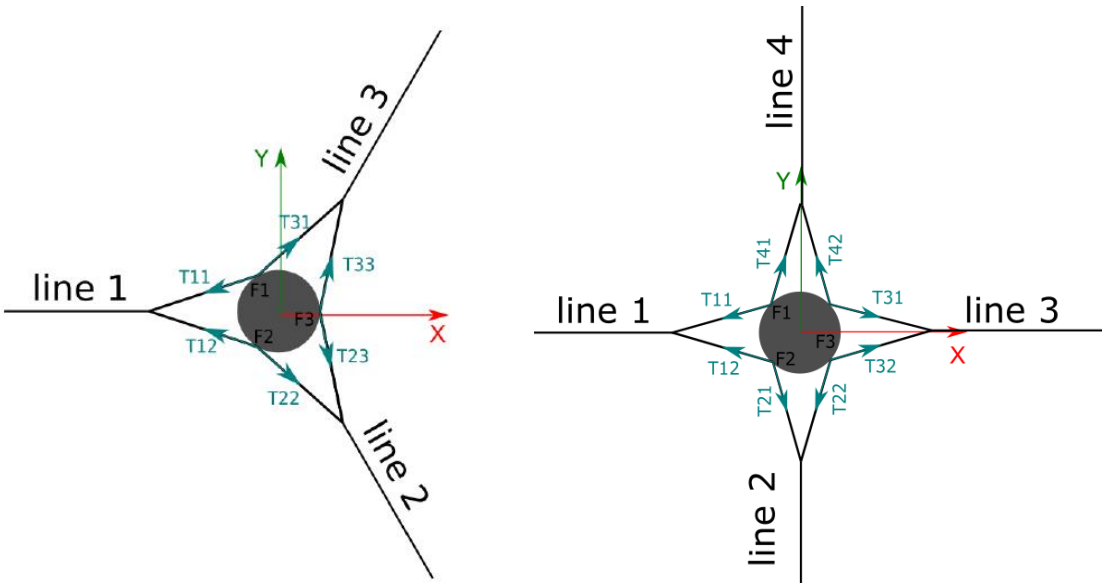

Figure 4-1: WindCrete fairlead configuration sketch with tension nomenclature for Gran Canaria (left) and Morro Bay (right)

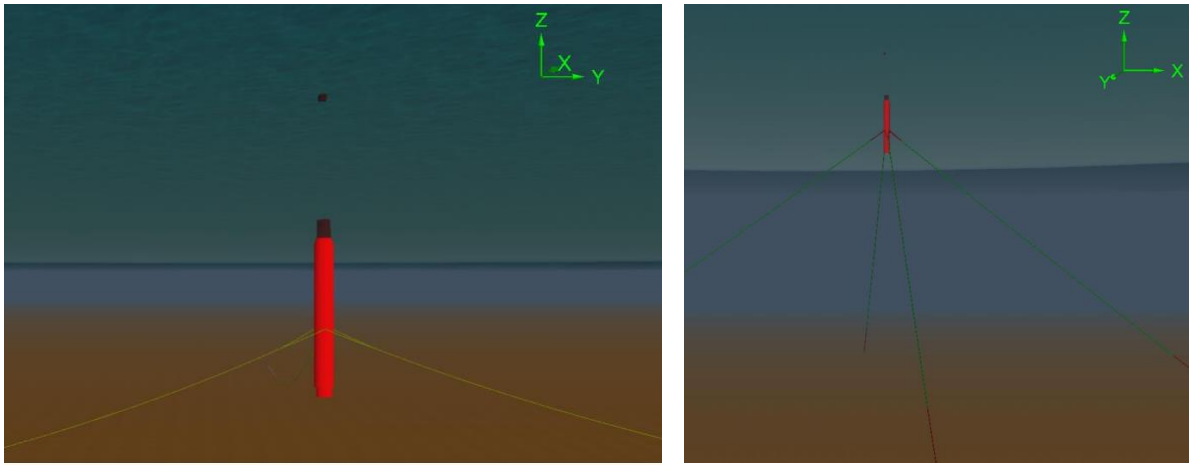

Figure 4-2: WindCrete Gran Canaria (Left) and Morro Bay (Right) mooring sketch

The Table 4-1 and Table 4-2 show the characteristics of the predesign and optimized mooring systems for the Gran Canaria and Morro Bay sites respectively. The optimized designs have smaller diameters for chain and synesthetic lines. The line lengths are increased for the Gran Canaria site whereas the line lengths are increased for the Morro Bay site.

Table 4-1: WindCrete Gran Canaria mooring system Predesign and Optimized characteristics

	Group of lines	Type of line	Chain bar diameter [mm]	Line Length [m]
PreDesign	**Upwind and Downwind lines**	Main line	160	565
		DeltaLines	160	50
Optimized	**Upwind lines**	Main line	111	700
		DeltaLines	111	50
	Downwind lines	Main Line	100	750
		DeltaLines	111	50

Table 4-2: WindCrete Morro Bay mooring system Predesign and Optimized characteristics

	Group of lines	Type of line	Material	Diameter [mm]	Line Length [m]
PreDesign	**Upwind and Downwind lines**	Main line	Chain	160	200
			Polyester	200	1078
		DeltaLines	Chain	120	50
Optimized	**Upwind lines**	Main line	Chain	102	195
			Polyester	193	1105
		DeltaLines	Chain	90	50
	Downwind lines	Main Line	Chain	95	180
			Polyester	205	1020
		DeltaLines	Chain	90	50

4.1.1.1 Gran Canaria results

The Table 4-3 and Table 4-4 show the result comparison for DLC 16 and DLC 61 respectively for Gran Canaria site. The tables show the maximum values for the platform motions, nacelle accelerations, tower base loads, mooring line tensions at the fairlead and the anchor tensions. The general trends of the simulations show that there is a mooring tension reductions. This can be seen in the tension reduction at the anchors and at the Fairleads which lead to a more economical solution. However, also a tension increase can be found for DLC16 at Fairlead 12. However, as the chain diameter of the predesign was not optimized, the optimized design shows to be a better solution. This increment can be associated to the large number of LCs analysed and that wind misalignment was included. Regarding the motions, the results are quite consistent with slight increase in pitch for the optimized design in DLC16 but a pitch reduction in DLC61. The Nacelle accelerations show a clear reduction for the optimized mooring systems for both DLCs. Also, the maximum bending moment is reduced for the optimized mooring system. These reductions can be attributed to a better integration between the mooring system and the platform motions.

DLC 16

Table 4-3: WindCrete Gran Canaria DLC1.6 simulation comparison

	Surge [m]	Sway [m]	Heave [m]	Roll [deg]	Pitch [deg]	Yaw [deg]
Predesign	13.2	5.1	1.5	3.0	5.5	8.3
Optimized	12.5	9.7	1.4	6.8	7.4	8.6
	Ax [m/s²]	**Ay [m/s²]**	**Az [m/s²]**			
Predesign	2.10	0.56	0.43			
Optimized	1.10	0.85	0.34			
	TwrBsMxt [kN·m]	**TwrBsMyt [kN·m]**	**TwrBsMzt [kN·m]**			
Predesign	2.79E+05	7.95E+05	6.93E+04			
Optimized	5.43E+05	6.23E+05	6.46E+04			
	FairTen11[N]	**FairTen12[N]**	**FairTen21[N]**	**FairTen22[N]**	**FairTen31[N]**	**FairTen32[N]**
Predesign	4.39E+06	4.48E+06	2.88E+06	3.85E+06	3.82E+06	2.86E+06
Optimized	3.70E+06	5.07E+06	2.64E+06	3.45E+06	2.59E+06	3.11E+06
	AnchTen1[N]	**AnchTen2[N]**	**AnchTen3[N]**			
Predesign	7.34E+06	4.31E+06	4.19E+06			
Optimized	6.66E+06	3.57E+06	3.79E+06			

DLC61

Table 4-4: WindCrete Gran Canaria DLC61 simulation comparison

	Surge [m]	Sway [m]	Heave [m]	Roll [deg]	Pitch [deg]	Yaw [deg]
Predesign	15.9	3.1	1.4	1.6	8.3	1.9
Optimized	3.0	3.5	0.9	1.6	1.4	1.4
	Ax [m/s²]	**Ay [m/s²]**	**Az [m/s²]**			
Predesign	1.45	0.52	0.23			
Optimized	0.21	0.21	0.05			
	TwrBsMxt [kN·m]	**TwrBsMyt [kN·m]**	**TwrBsMzt [kN·m]**			
Predesign	1.44E+05	7.27E+05	1.55E+04			
Optimized	1.68E+05	1.32E+05	1.13E+04			
	FairTen11[N]	**FairTen12[N]**	**FairTen21[N]**	**FairTen22[N]**	**FairTen31[N]**	**FairTen32[N]**
Predesign	3.79E+06	4.02E+06	3.19E+06	2.27E+06	3.28E+06	2.11E+06
Optimized	2.77E+06	2.75E+06	2.33E+06	2.14E+06	2.13E+06	2.31E+06
	AnchTen1[N]	**AnchTen2[N]**	**AnchTen3[N]**			
Predesign	6.61E+06	4.10E+06	4.10E+06			
Optimized	4.85E+06	3.87E+06	3.89E+06			

4.1.1.2 Morro Bay results

Morro Bay results comparison in Table 4-5 and Table 4-6 for DLC16 and 61 respectively show an increase of the mooring tension at both anchor and fairleads. However, the Nacelle accelerations and tower base moments present a clear reduction of the maximum values. The different behaviour between the Gran Canaria simulations and the Morro Bay ones can be explained because of the different nature of the mooring system, a catenary

mooring system for Gran Canaria and a taut mooring system for Morro Bay. The optimization process in Morro Bay lead to a more loaded mooring system but which performs better in terms of strength/cost and also improves the platform behaviour in terms of motions, accelerations and tower base loads.

DLC 16

Table 4-5: WindCrete Morro Bay DLC16 simulation comparison

	Surge [m]	Sway [m]	Heave [m]	Roll [deg]	Pitch [deg]	Yaw [deg]
Predesign	21.0	4.6	2.9	2.0	5.1	6.2
Optimized	20.3	5.7	0.9	3.1	4.4	6.5
	Ax [m/s²]	**Ay [m/s²]**	**Az [m/s²]**			
Predesign	2.76	0.48	0.43			
Optimized	1.18	0.72	0.24			
	TwrBsMxt [kN·m]	**TwrBsMyt [kN·m]**	**TwrBsMzt [kN·m]**			
Predesign	2.01E+05	1.07E+06	5.38E+04			
Optimized	2.87E+05	5.32E+05	7.67E+04			
	FairTen11 [N]	**FairTen12 [N]**	**FairTen21 [N]**	**FairTen22 [N]**	**FairTen31 [N]**	**FairTen32[N]**	**FairTen41 [N]**	**FairTen42 [N]**
Predesign	3.44E+06	4.05E+06	2.91E+06	3.34E+06	2.49E+06	3.10E+06	2.68E+06	3.55E+06
Optimized	3.68E+06	4.11E+06	3.80E+06	4.40E+06	2.96E+06	3.97E+06	3.42E+06	4.47E+06
	AnchTen1 [N]	**AnchTen2 [N]**	**AnchTen3 [N]**	**AnchTen4 [N]**				
Predesign	5.94E+06	3.68E+06	3.57E+06	3.81E+06				
Optimized	6.92E+06	5.57E+06	5.09E+06	5.52E+06				

DLC61

Table 4-6: WindCrete Morro Bay DLC61 simulation comparison

	Surge [m]	Sway [m]	Heave [m]	Roll [deg]	Pitch [deg]	Yaw [deg]
Predesign	21.4	2.8	2.5	1.1	7.4	2.1
Optimized	9.9	4.2	1.6	1.6	2.5	1.6
	Ax [m/s²]	**Ay [m/s²]**	**Az [m/s²]**			
Predesign	2.49	0.65	0.43			
Optimized	0.48	0.50	0.12			
	TwrBsMxt [kN·m]	**TwrBsMyt [kN·m]**	**TwrBsMzt [kN·m]**			
Predesign	1.67E+05	9.18E+05	1.52E+04			
Optimized	1.97E+05	1.87E+05	1.50E+04			

	FairTen11 [N]	FairTen12 [N]	FairTen21 [N]	FairTen22 [N]	FairTen31 [N]	FairTen32 [N]	FairTen41 [N]	FairTen42 [N]
Predesign	3.40E+06	3.46E+06	3.43E+06	2.32E+06	2.24E+06	2.58E+06	2.20E+06	3.56E+06
Optimized	3.26E+06	3.35E+06	3.54E+06	3.37E+06	3.04E+06	3.08E+06	3.27E+06	3.70E+06

	AnchTen1 [N]	AnchTen2 [N]	AnchTen3 [N]	AnchTen4 [N]
Predesign	5.49E+06	3.83E+06	3.63E+06	3.96E+06
Optimized	5.93E+06	5.96E+06	5.21E+06	6.05E+06

4.1.2 ActiveFloat mooring system designs

ActiveFloat design comparison is performed for Gran Canaria and Morro Bay locations. West of Barra location was disregarded due to the large difference between the predesign one, with three mooring lines, with the optimized one with 12 mooring lines. It is worth to notice that the predesign mooring system did not fulfil the DLC requirements for a final design. The Figure 4-3 shows and sketch of the mooring line configuration of ActiveFloat and its nomenclature.

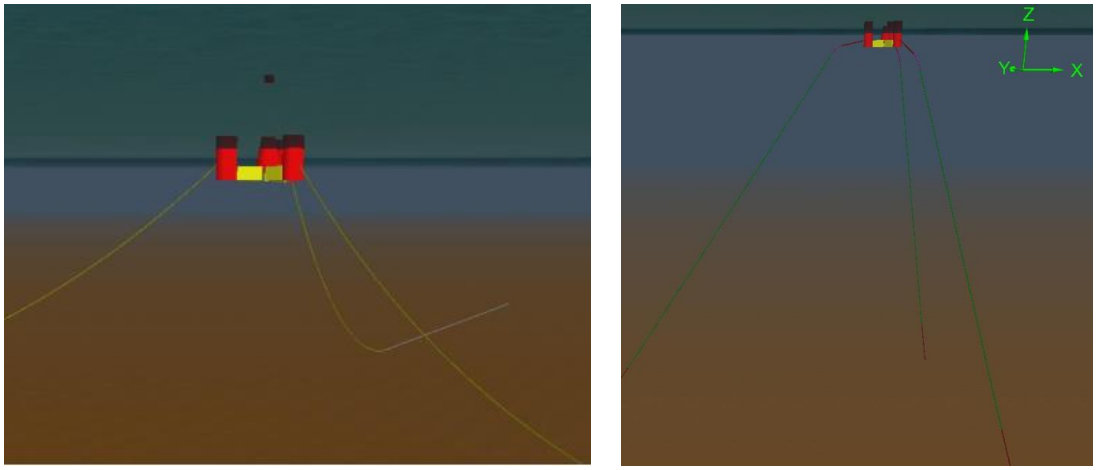

Figure 4-3:Active Float Gran Canaria (Left) and Morro Bay (Right) mooring sketch

The Figure 4-7Table 4-7 and Table 4-8 show the characteristics of the predesign and optimized mooring systems for the Gran Canaria and Morro Bay sites respectively. The optimized designs have smaller chain diameters and longer line lengths for Gran Canaria site. For Morro Bay site the optimized designs present smaller chain diameters, the synthetic line diameters are larger for the upwind lines, and the total line length are shorter.

Table 4-7: ActiveFloat Gran Canaria mooring system Predesign and Optimized characteristics

	Group of lines	Chain bar diameter [mm]	Line Length [m]
PreDesign	**Upwind and Downwind lines**	160	614
Optimized	**Upwind lines**	120	832
	Downwind lines	70	832

Table 4-8: ActiveFloat Morro Bay mooring system Predesign and Optimized characteristics

	Group of lines	Material	Diameter [mm]	Line Length [m]
PreDesign	**Upwind and Downwind lines**	Chain	301	200
		Polyester	153	1100
		Chain	128	50
Optimized	**Upwind lines**	Chain	128	200
		Polyester	196	850
	Downwind lines	Chain	92	181.25
		Polyester	146	743.75

4.1.2.1 Gran Canaria Results

The mooring system comparison results for DLC 16 and 61 for Gran Canaria are shown in Table 4-9 and Table 4-10 respectively. The results shows a mooring tension reduction for the optimized design. On the other hand, the results also shows a more compliant design for the optimized one with large platform motions and slight larger acceleration. However, the tower loads are reduced in both DLC, 16 and 61 for the optimized mooring system design.

DLC1.6

Table 4-9: ActiveFloat Gran Canaria DLC1.6 simulation comparison

	Surge [m]	Sway [m]	Heave [m]	Roll [deg]	Pitch [deg]	Yaw [deg]
Predesign	20.4	3.0	0.9	2.6	4.0	11.7
Optimized	50.9	32.0	0.4	5.0	4.7	28.6
	Ax [m/s²]	**Ay [m/s²]**	**Az [m/s²]**			
Predesign	1.5	0.8	0.6			
Optimized	2.0	1.0	0.7			
	TwrBsMxt [kN·m]	**TwrBsMyt [kN·m]**	**TwrBsMzt [kN·m]**			
Predesign	2.07E+05	4.70E+05	6.52E+04			
Optimized	2.80E+05	4.52E+05	7.07E+04			
	FairTen1[N]	**FairTen2[N]**	**FairTen3[N]**			
Predesign	6.23E+06	2.97E+06	3.08E+06			
Optimized	4.99E+06	6.94E+05	5.71E+05			

DLC.61

Table 4-10: ActiveFloat Gran Canaria DLC61 simulation comparison

	Surge [m]	Sway [m]	Heave [m]	Roll [deg]	Pitch [deg]	Yaw [deg]
Predesign	16.5	5.8	1.0	1.9	3.4	2.5
Optimized	42.7	22.5	0.4	2.1	3.1	5.8
	Ax [m/s²]	**Ay [m/s²]**	**Az [m/s²]**			
Predesign	0.9	0.5	0.4			
Optimized	0.6	0.8	0.6			
	TwrBsMxt [kN·m]	**TwrBsMyt [kN·m]**	**TwrBsMzt [kN·m]**			
Predesign	1.29E+05	2.65E+05	1.24E+04			
Optimized	1.37E+05	1.77E+05	1.14E+04			
	FairTen1[N]	**FairTen2[N]**	**FairTen3[N]**			
Predesign	5.24E+06	3.07E+06	3.15E+06			
Optimized	3.32E+06	6.11E+05	5.94E+05			

4.1.2.2 Morro Bay Results

The results of the simulation comparison for DLC16 and 61 or Morro Bay site are shown in Table 4-11 and Table 4-12 respectively. In this case the optimized mooring system also shows a tension reduction of the mooring lines. Also, the motions of the platform are more compliant for the translation. The rotations slightly increase or decrease depending on the direction and DLC, but it can be seen that the Yaw for DLC16 is much larger which could also mean a more compliant design for the optimized mooring system than the predesign one. In this case the nacelle accelerations and the tower base loads are reduced.

DLC1.6

Table 4-11: ActiveFloat Morro Bay DLC16 simulation comparison

	Surge [m]	Sway [m]	Heave [m]	Roll [deg]	Pitch [deg]	Yaw [deg]
Predesign	22.6	2.6	3.1	1.7	4.2	9.8
Optimized	51.9	29.4	2.4	3.1	3.2	32.1
	Ax [m/s²]	**Ay [m/s²]**	**Az [m/s²]**			
Predesign	1.88	0.82	0.86			
Optimized	1.45	0.84	0.69			
	TwrBsMxt [kN·m]	**TwrBsMyt [kN·m]**	**TwrBsMzt [kN·m]**			
Predesign	1.97E+05	5.06E+05	5.40E+04			
Optimized	2.05E+05	4.52E+05	6.32E+04			
	FairTen1[N]	**FairTen2[N]**	**FairTen3[N]**			
Predesign	6.23E+06	3.09E+06	2.98E+06			
Optimized	5.13E+06	1.35E+06	1.53E+06			

DLC6.1

Table 4-12: ActiveFloat Morro Bay DLC61 simulation comparison

	Surge [m]	Sway [m]	Heave [m]	Roll [deg]	Pitch [deg]	Yaw [deg]
Predesign	19.9	3.8	2.9	1.4	3.2	2.7
Optimized	13.2	38.1	2.8	4.3	2.3	4.9
	Ax [m/s²]	**Ay [m/s²]**	**Az [m/s²]**			
Predesign	1.31	0.44	0.62			
Optimized	0.64	0.56	0.43			
	TwrBsMxt [kN·m]	**TwrBsMyt [kN·m]**	**TwrBsMzt [kN·m]**			
Predesign	1.23E+05	2.86E+05	1.32E+04			
Optimized	3.53E+05	1.84E+05	1.76E+04			
	FairTen1[N]	**FairTen2[N]**	**FairTen3[N]**			
Predesign	6.03E+06	3.01E+06	3.08E+06			
Optimized	3.37E+06	2.37E+06	2.15E+06			

4.2 Peak Reduction System influence on mooring systems

This section gives some conclusions regarding the influence on the mooring system, of the use of peak loads reduction systems attached to the mooring lines. Two systems have been considered for performing mooring optimizations and simulations corresponding to DLC 6.1 and 6.2. The systems are named System 1 and System 2 for confidentiality reasons. Both systems are featuring a variable stiffness but have different approaches regarding shock absorption. More information is given in deliverable D2.3.

Results of maximum platform offsets and maximum fairlead tensions are given for DLC6.1 and 6.2, with WindCrete and ActiveFloat floaters at site B (Gran Canaria) and site C (Morro Bay). The peak load reduction systems have been attached to the top section of the mooring lines from the initial mooring systems (non-

optimized). Then, the python optimization tool has been used to optimize the moorings equipped with System 1 and System 2. The objective was to minimize the total cost of materials, varying the line diameters, the chain grades, the line lengths, as well as the peak load reduction systems properties and number of units per line. Detailed information on the optimized moorings is given in deliverable D2.3.

4.2.1 WindCrete mooring system at site B (Gran Canaria)

In the following tables are presented, for the three mooring systems of WindCrete at Gran Canaria (without PLRS, with System 1 and with System 2), the results of maximum platform offsets, maximum vertical and horizontal accelerations of the nacelle and maximum displacements and loads in the 3 directions, of the connections (between the delta-lines linked to the floater and the main-lines linked to the anchor) and the fairleads. Positions of the connections and fairleads 1, 2 and 3 are illustrated in Figure 4-4 and Figure 4-5. The displacements are given with respect to the static positions.

Gran Canaria results of maximum platform offsets and nacelle accelerations for WindCrete						
Peak loads reduction system	**0**	**System 1**	**System 2**	**0**	**System 1**	**System 2**
DLC	**6.1**	**6.1**	**6.1**	**6.2**	**6.2**	**6.2**
Max offset (m)	5.6	5.5	5.0	7.8	8.0	7.3
Max vertical nacelle acceleration (m/s2)	0.1	0.1	0.2	0.1	0.1	0.2
Max horizontal acceleration (m/s2)	1.6	1.6	1.6	1.6	1.6	1.6

Table 4-13 Maximum offsets and nacelle accelerations, WindCrete Gran Canaria

Regarding the maximum offsets and nacelle accelerations, the differences observed are considered not relevant. For each of the mooring systems, similar magnitudes are observed.

Gran Canaria results of maximum fairleads offsets for WindCrete						
Peak loads reduction system	**0**	**System 1**	**System 2**	**0**	**System 1**	**System 2**
DLC	**6.1**	**6.1**	**6.1**	**6.2**	**6.2**	**6.2**
Maximum X (m) connection 1	2.8	4.7	3.6	3.4	6.2	4.8
Maximum X (m) connection 2	9.8	13.4	13.0	14.1	16.3	15.6
Maximum X (m) connection 3	10.6	13.4	12.5	13.3	16.9	16.2
Maximum X (m) fairlead 1	4.8	9.9	9.7	9.6	14.2	13.8
Maximum X (m) fairlead 2	-0.6	-0.2	-0.4	-0.5	0.6	0.2
Maximum X (m) fairlead 3	3.2	6.5	6.8	5.1	9.5	9.0
Maximum Y (m) connection 1	3.5	2.9	2.0	4.0	3.0	2.9
Maximum Y (m) connection 2	-2.6	-2.0	-1.7	-2.5	-1.7	-1.5
Maximum Y (m) connection 3	-1.7	-1.8	-1.6	-1.6	-1.6	-1.4
Maximum Y (m) fairlead 1	2.9	3.6	3.1	3.4	5.0	4.2
Maximum Y (m) fairlead 2	5.8	7.4	6.5	6.6	9.0	7.7
Maximum Y (m) fairlead 3	2.8	3.9	3.1	3.3	5.1	4.2
Maximum Z (m) connection 1	-0.5	0.5	0.5	0.0	1.4	1.2
Maximum Z (m) connection 2	2.1	4.3	3.7	3.6	5.6	4.9
Maximum Z (m) connection 3	1.8	3.6	3.3	3.2	4.6	4.1
Maximum Z (m) fairlead 1	-0.3	-0.3	-0.3	-0.4	-0.5	-0.5
Maximum Z (m) fairlead 2	-0.8	-0.5	-0.6	-1.0	-0.7	-0.8
Maximum Z (m) fairlead 3	-0.2	-0.3	-0.4	-0.4	-0.5	-0.5

Table 4-14 Maximum fairleads and connections displacements, WindCrete Gran Canaria

Fairlead and connection displacements with respect to their position in the static state are all of similar magnitudes, so that conclusions would not be relevant at this stage.

In the following table are presented the maximum tensions in the three directions for the three fairleads. In addition are listed the maximum resulting tensions at the three connections between the delta lines and the main line.

Gran Canaria results of maximum fairleads loads for WindCrete						
Peak loads reduction system	**0**	**System 1**	**System 2**	**0**	**System 1**	**System 2**
DLC	**6.1**	**6.1**	**6.1**	**6.2**	**6.2**	**6.2**
Maximum Tx (kN) connection 1	-11217.7	-6155.4	-6281.4	-11332.2	-6234.3	-6280.9
Maximum Tx (kN) connection 2	5042.6	2691.5	2756.1	5137.4	2773.9	2808.7
Maximum Tx (kN) connection 3	5161.0	2682.6	2718.2	5179.0	2793.8	2827.7
Maximum Tx (kN) fairlead 1	122.7	82.2	97.9	217.5	133.3	163.5
Maximum Tx (kN) fairlead 2	-7361.2	-3968.8	-3896.2	-7269.3	-3853.8	-3796.0
Maximum Tx (kN) fairlead 3	8738.6	4617.5	4619.5	8826.1	4739.6	4814.1
Maximum Ty (kN) connection 1	-4159.3	-1869.6	-2132.7	-4156.5	-1935.9	-2128.9
Maximum Ty (kN) connection 2	-3277.9	-1393.0	-1211.1	-3252.7	-1373.9	-1193.5
Maximum Ty (kN) connection 3	-3328.0	-1398.8	-1214.8	-3290.1	-1374.0	-1193.0
Maximum Ty (kN) fairlead 1	-1512.1	-873.3	-877.3	-1405.7	-866.0	-891.1
Maximum Ty (kN) fairlead 2	1630.4	901.2	878.8	1610.4	903.8	894.8
Maximum Ty (kN) fairlead 3	-1509.7	-892.4	-923.1	-1470.2	-849.9	-871.9
Maximum Tz (kN) connection 1	-1366.1	-679.9	-684.9	-1329.6	-662.0	-673.6
Maximum Tz (kN) connection 2	1051.8	693.6	740.3	1385.9	1139.7	1215.3
Maximum Tz (kN) connection 3	2092.9	1114.2	1189.1	2429.0	1348.9	1484.6
Maximum Tz (kN) fairlead 1	-2225.4	-920.2	-938.6	-2227.6	-920.8	-930.8
Maximum Tz (kN) fairlead 2	-1998.7	-827.8	-716.0	-1961.1	-812.7	-701.6
Maximum Tz (kN) fairlead 3	-2255.8	-928.6	-941.2	-2254.6	-921.2	-929.4

Table 4-15 Maximum loads at the fairleads and connections, WindCrete Gran Canaria

Regarding the loads it is interesting to note that in all directions and for all the connections and fairleads, the magnitudes are 50% lower when the mooring systems are equipped with PLRS (System 1 and System 2). Also, no relevant differences are observed between the loads of the moorings equipped with System 1 or System 2.

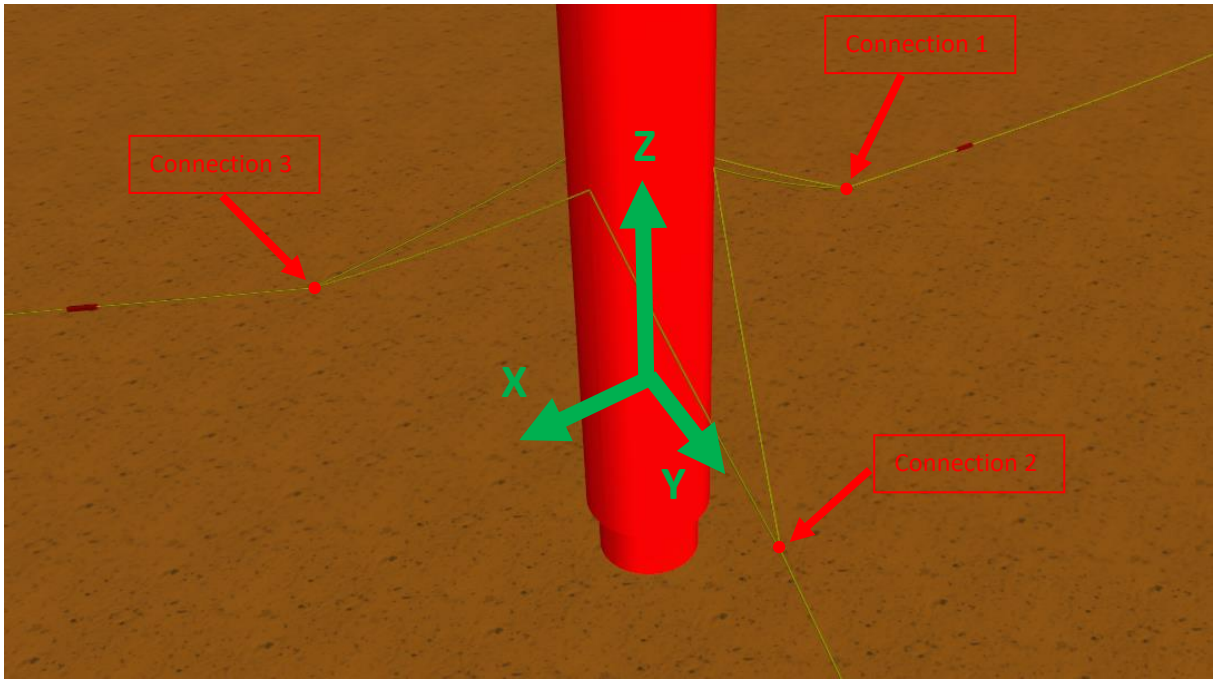

Figure 4-4 Illustration of the locations of the three connections and the axes.

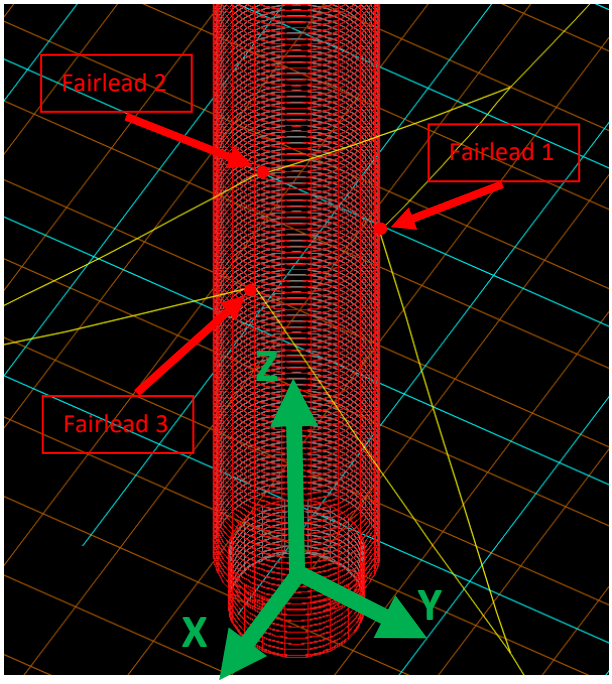

Figure 4-5 Illustration of the location of the three fairleads

4.2.2 WindCrete mooring system at site C (Morro Bay)

In the following tables are presented, for the three mooring systems of WindCrete at Morro Bay (without PLRS, with System 1 and with System 2), the results of maximum platform offsets, maximum vertical and horizontal accelerations of the nacelle and maximum displacements and loads in the 3 directions, of the connections (between the delta-lines linked to the floater and the main-lines linked to the anchor) and the fairleads. Positions of the four connections and three fairleads are illustrated in Figure 4-6 and Figure 4-7. The displacements are given with respect to the static positions.

Morro Bay results of maximum platform offsets and nacelle accelerations for WindCrete						
Peak loads reduction system	**0**	**System 1**	**System 2**	**0**	**System 1**	**System 2**
DLC	**6.1**	**6.1**	**6.1**	**6.2**	**6.2**	**6.2**
Max offset (m)	9.9	7.9	7.8	13.2	15.2	14.5
Max vertical nacelle acceleration (m/s2)	0.4	0.4	0.4	0.4	0.4	0.4
Max horizontal acceleration (m/s2)	3.1	2.6	2.6	2.4	2.4	2.4

Table 4-16 Maximum offsets and nacelle accelerations, WindCrete Morro Bay

For each of the mooring systems, similar magnitudes are observed when looking at the maximum offsets and nacelle accelerations.

Morro Bay results of maximum fairleads offsets for WindCrete						
Peak loads reduction system	**0**	**System 1**	**System 2**	**0**	**System 1**	**System 2**
DLC	**6.1**	**6.1**	**6.1**	**6.2**	**6.2**	**6.2**
Maximum X (m) connection 1	9.9	7.9	7.8	15.2	15.2	14.5
Maximum X (m) connection 2	0.4	0.4	0.4	0.4	0.4	0.4
Maximum X (m) connection 3	3.1	2.6	2.6	2.4	2.4	2.4
Maximum X (m) connection 4	-4.9	-4.4	-4.8	0.0	0.0	-2.0
Maximum X (m) fairlead 1	16.3	11.7	-4.1	32.7	32.7	-2.1
Maximum X (m) fairlead 2	13.8	11.3	10.9	25.3	25.3	21.7
Maximum X (m) fairlead 3	16.1	11.9	-4.1	32.8	32.8	-1.9
Maximum X (m) fairlead 4	16.4	8.4	8.9	29.5	29.5	28.4
Maximum Y (m) connection 1	-1.2	-0.1	-0.1	2.5	2.5	2.9
Maximum Y (m) connection 2	16.9	8.3	9.9	27.5	27.5	26.5
Maximum Y (m) connection 3	10.4	5.6	5.5	18.9	18.9	19.0
Maximum Y (m) connection 4	-4.2	-4.4	-4.1	-3.9	-3.9	-3.8
Maximum Y (m) fairlead 1	-3.5	-4.1	-4.0	-3.8	-3.7	-3.8
Maximum Y (m) fairlead 2	-3.9	-4.1	-4.0	-4.6	-4.4	-4.5
Maximum Y (m) fairlead 3	-4.0	-4.1	-4.0	-3.8	-3.7	-3.8
Maximum Y (m) fairlead 4	-3.6	-3.1	-3.3	0.2	0.2	-1.5
Maximum Z (m) connection 1	9.3	7.9	7.4	17.5	17.5	14.8
Maximum Z (m) connection 2	9.0	7.9	7.4	17.3	17.3	15.0
Maximum Z (m) connection 3	-3.4	-3.3	-3.4	0.2	0.2	-1.5
Maximum Z (m) connection 4	-1.2	0.0	0.0	1.1	1.1	1.4
Maximum Z (m) fairlead 1	-1.5	0.0	0.0	1.0	1.0	1.2
Maximum Z (m) fairlead 2	7.3	3.7	3.8	13.6	13.6	13.3
Maximum Z (m) fairlead 3	7.3	3.7	3.7	13.2	13.2	13.6
Maximum Z (m) fairlead 4	-2.4	-2.6	-2.6	-2.5	-2.5	-2.6

Table 4-17 Maximum fairleads and connections displacements, WindCrete Morro Bay

Fairlead and connection displacements with respect to their position in the static state are all of similar magnitudes, so that conclusions would not be relevant at this stage.

In the following table are presented the maximum tensions in the three directions for the three fairleads. In addition are listed the maximum resulting tensions at the three connections between the delta lines and the main line.

Morro Bay results of maximum fairleads loads for WindCrete						
Peak loads reduction system	**0**	**System 1**	**System 2**	**0**	**System 1**	**System 2**
DLC	**6.1**	**6.1**	**6.1**	**6.2**	**6.2**	**6.2**
Maximum Tx (kN) connection 1	-6786.0	-6917.9	-7402.0	-6974.9	-6969.7	-7456.8
Maximum Tx (kN) connection 2	199.1	-37.2	127.8	238.7	238.7	364.0
Maximum Tx (kN) connection 3	7673.7	7547.4	7840.5	7530.4	7530.4	7813.0
Maximum Tx (kN) connection 4	208.4	-37.2	119.7	218.5	218.5	345.7
Maximum Tx (kN) fairlead 1	182.3	81.3	84.2	307.5	307.5	440.5
Maximum Tx (kN) fairlead 2	-6417.9	-7146.9	-6294.3	-6915.9	-6888.8	-6058.5
Maximum Tx (kN) fairlead 3	181.6	69.8	89.9	296.2	296.2	397.2
Maximum Tx (kN) fairlead 4	8044.3	7822.0	6936.7	8676.2	8676.2	7834.6
Maximum Ty (kN) connection 1	-4803.8	-4731.3	-4879.7	-4759.5	-4740.5	-4910.0
Maximum Ty (kN) connection 2	-5150.2	-5337.9	-4539.1	-5179.6	-5162.6	-4372.0
Maximum Ty (kN) connection 3	-5432.9	-5180.1	-5142.5	-4901.5	-4900.3	-5018.0
Maximum Ty (kN) connection 4	-5264.5	-5337.9	-4539.1	-5182.4	-5171.5	-4371.0
Maximum Ty (kN) fairlead 1	-1680.8	-1412.3	-1535.3	-1523.5	-1517.2	-1666.8
Maximum Ty (kN) fairlead 2	2492.3	1933.1	2191.8	2845.6	2845.6	3152.2
Maximum Ty (kN) fairlead 3	2470.7	1916.5	2183.6	3009.7	3009.7	3269.0
Maximum Ty (kN) fairlead 4	-1687.4	-1412.3	-1535.3	-1478.9	-1476.2	-1628.6
Maximum Tz (kN) connection 1	-1649.4	-1577.8	-1370.8	-1657.6	-1652.2	-1469.1
Maximum Tz (kN) connection 2	-1704.3	-1603.7	-1317.1	-1643.6	-1637.4	-1372.1
Maximum Tz (kN) connection 3	2712.3	2219.4	1937.6	3436.7	3436.7	3084.4
Maximum Tz (kN) connection 4	2511.3	2197.3	2033.0	3729.5	3729.5	3414.1
Maximum Tz (kN) fairlead 1	-2743.4	-2649.4	-2530.1	-2610.9	-2602.6	-2520.7
Maximum Tz (kN) fairlead 2	-2904.0	-2799.1	-2569.7	-2718.7	-2703.2	-2521.6
Maximum Tz (kN) fairlead 3	-2924.2	-2799.1	-2569.7	-2719.8	-2705.9	-2525.9
Maximum Tz (kN) fairlead 4	-2778.9	-2649.4	-2530.1	-2624.5	-2619.9	-2519.8

Table 4-18 Maximum loads at the fairleads and connections, WindCrete Morro Bay

When looking at the loads at the connections and fairleads, small discrepancies are observed between the three mooring systems. The most important loads are observed in the X-direction at connection 3 and fairlead 4.

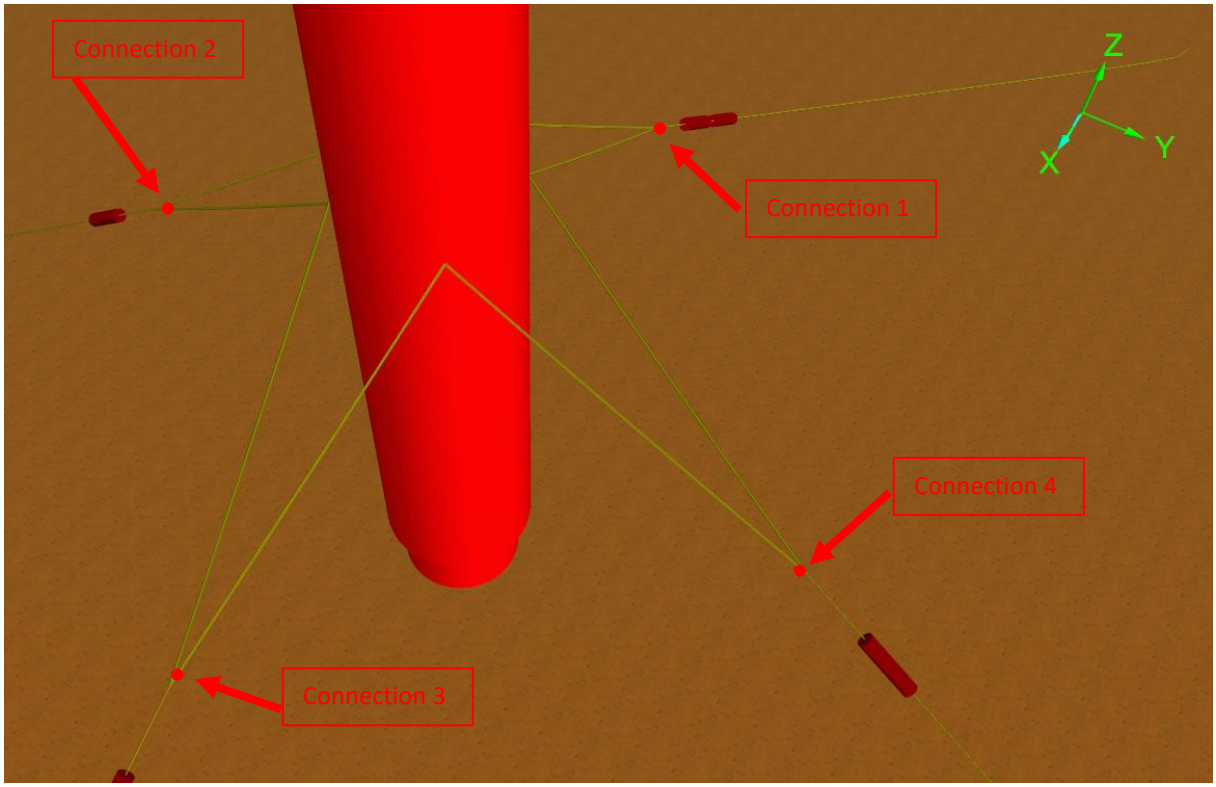

Figure 4-6 Illustration of the locations of the four connections

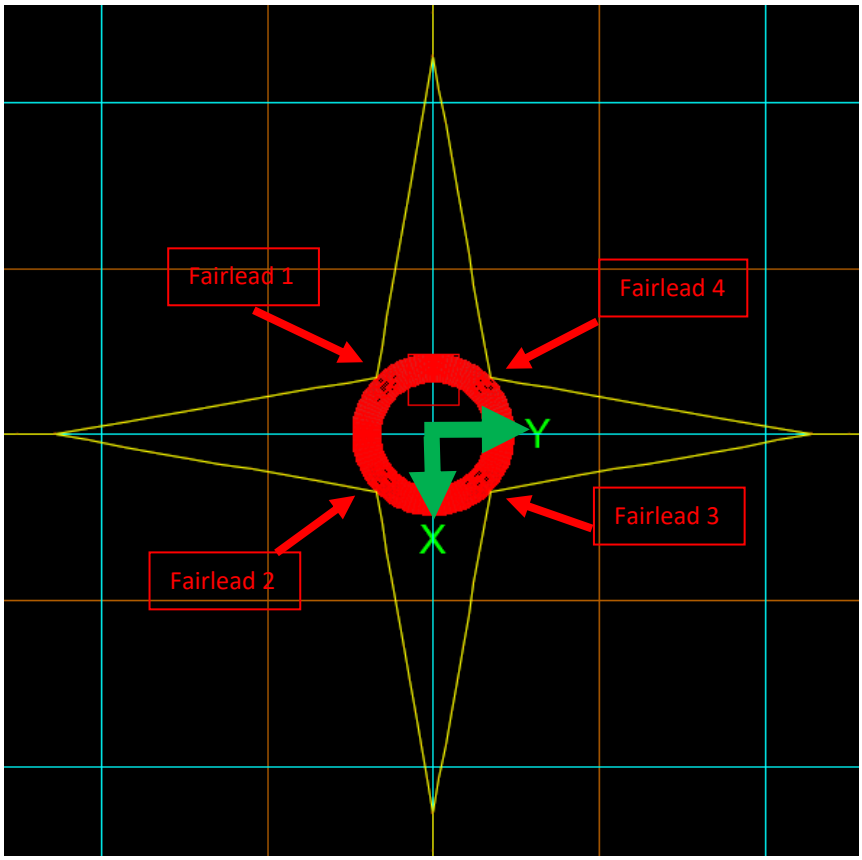

Figure 4-7 Illustration of the location of the four fairleads

4.2.3 ActiveFloat mooring system at site B (Gran Canaria)

Here are presented, for the three mooring systems of ActiveFloat at Gran Canaria (without PLRS, with System 1 and with System 2), the results of maximum platform offsets, maximum vertical and horizontal accelerations of the nacelle and maximum displacements and loads in the 3 directions, of the fairleads. Positions of the three fairleads are illustrated in Figure 4-8. The displacements are given with respect to the static positions.

Gran Canaria results of maximum platform offsets, nacelle accelerations and mooring tensions for ActiveFloat						
Peak loads reduction system	**0**	**System 1**	**System 2**	**0**	**System 1**	**System 2**
DLC	**6.1**	**6.1**	**6.1**	**6.2**	**6.2**	**6.2**
Max offset (m)	63.2	58.2	57.2	66.8	57.2	56.3
Max vertical nacelle acceleration (m/s2)	0.4	0.4	0.5	0.7	0.4	0.5
Max horizontal acceleration (m/s2)	1.6	0.7	1.5	3.3	0.7	0.9
Maximum X (m) fairlead 1	33.3	24.4	24.4	35.9	26.0	25.5
Maximum X (m) fairlead 2	33.5	39.7	38.4	36.1	38.1	38.2
Maximum X (m) fairlead 3	33.6	40.6	39.3	36.1	38.1	39.1
Maximum Y (m) fairlead 1	34.8	44.6	44.3	44.1	44.8	43.2
Maximum Y (m) fairlead 2	16.1	22.7	20.1	22.6	26.3	25.6
Maximum Y (m) fairlead 3	35.9	46.8	46.6	46.2	46.3	45.6
Maximum Z (m) fairlead 1	-0.6	-1.1	-1.1	0.1	-0.8	-1.1
Maximum Z (m) fairlead 2	-0.9	-0.4	-0.3	-0.7	-0.3	-0.3
Maximum Z (m) fairlead 3	-0.6	-0.4	-0.3	-0.4	-0.2	-0.3
Maximum Tx (kN) fairlead 1	-2829.7	-2195.8	-2189.1	-3165.2	-2235.5	-2210.0
Maximum Tx (kN) fairlead 2	622.5	573.4	610.8	736.3	566.6	610.8
Maximum Tx (kN) fairlead 3	714.2	545.3	467.0	807.6	549.4	543.9
Maximum Ty (kN) fairlead 1	216.9	143.7	119.8	254.1	137.7	134.2
Maximum Ty (kN) fairlead 2	-383.0	-103.1	-99.0	-339.3	-85.5	-99.0
Maximum Ty (kN) fairlead 3	1031.6	783.6	645.0	1167.3	783.7	764.7
Maximum Tz (kN) fairlead 1	-2409.3	-1205.3	-1227.3	-2488.7	-1215.3	-1227.3
Maximum Tz (kN) fairlead 2	-744.3	-197.5	-162.1	-718.6	-189.4	-162.1
Maximum Tz (kN) fairlead 3	-789.7	-195.7	-168.4	-747.5	-189.7	-168.4

Table 4-19 Maximum offsets, nacelle accelerations, fairlead displacements and loads, ActiveFloat Gran Canaria

It is interesting to note that the maximum offsets of the platform are reduced of almost 10% when using System 1 or System 2 in the mooring system. Also, the maximum horizontal accelerations observed with the initially optimized mooring system were reaching a critical value of 3.3m/s2, which is reduced to a value of 0.7m/s2 and 1.5m/s2 respectively for the mooring equipped with System 1 and with System 2.

Regarding the loads, maximum values reached for fairlead 1 in the X-direction are reduced of 20% when PLRS are used (System 1 or System 2). In the other directions, the maximum loads are reduced of 50%.

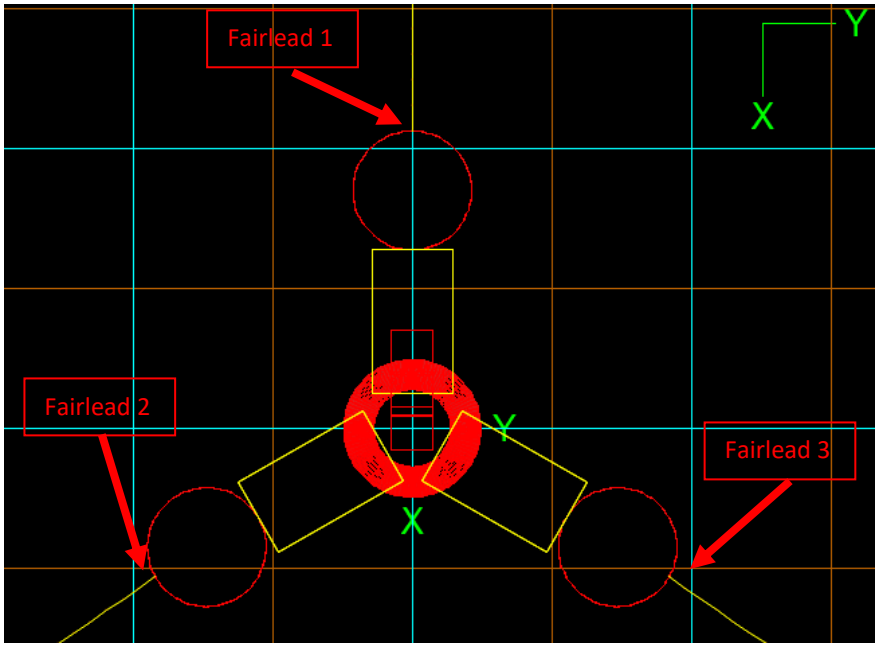

Figure 4-8 Illustration of the location of the three fairleads

4.2.4 ActiveFloat mooring system at site C (Morro Bay)

Here are presented, for the three mooring systems of ActiveFloat at Morro Bay (without PLRS, with System 1 and with System 2), the results of maximum platform offsets, maximum vertical and horizontal accelerations of the nacelle and maximum displacements and loads in the 3 directions, of the fairleads. Positions of the three fairleads are illustrated in Figure 4-9. The displacements are given with respect to the static positions.

Morro Bay results of maximum platform offsets and nacelle accelerations for ActiveFloat						
Peak loads reduction system	**0**	**System 1**	**System 2**	**0**	**System 1**	**System 2**
DLC	**6.1**	**6.1**	**6.1**	**6.2**	**6.2**	**6.2**
Max offset (m)	46.8	38.6	30.2	47.4	44.1	32.0
Max vertical nacelle acceleration (m/s^2)	1.1	1.0	1.0	0.7	0.9	0.9
Max horizontal acceleration (m/s^2)	2.1	3.4	3.3	1.6	3.0	3.0
Maximum X (m) fairlead 1	4.3	2.8	-0.6	12.7	10.7	5.6
Maximum X (m) fairlead 2	27.9	24.0	20.1	29.1	30.5	24.1
Maximum X (m) fairlead 3	28.3	23.8	19.9	28.7	30.5	23.8
Maximum Y (m) fairlead 1	32.2	32.7	24.9	39.0	38.5	26.1
Maximum Y (m) fairlead 2	31.6	33.5	24.4	38.1	38.1	26.2
Maximum Y (m) fairlead 3	15.3	12.9	7.2	21.5	20.2	11.6
Maximum Z (m) fairlead 1	-3.4	-2.9	-3.0	-3.2	-2.5	-2.5
Maximum Z (m) fairlead 2	-1.5	0.2	0.2	-1.9	-0.4	-0.5
Maximum Z (m) fairlead 3	-1.7	0.1	0.0	-1.9	-0.5	-0.6
Maximum Tx (kN) fairlead 1	-2041.0	-2063.9	-2542.3	-2028.8	-2061.7	-2539.7
Maximum Tx (kN) fairlead 2	1156.4	1184.2	1451.4	1164.2	1240.7	1521.5
Maximum Tx (kN) fairlead 3	1127.8	1181.0	1474.8	1163.0	1219.0	1503.6
Maximum Ty (kN) fairlead 1	276.0	228.3	271.6	351.8	314.5	315.9
Maximum Ty (kN) fairlead 2	1690.6	1668.2	2136.8	1799.5	1893.0	2316.6
Maximum Ty (kN) fairlead 3	-987.4	-1070.9	-1496.7	-922.0	-970.2	-1400.3
Maximum Tz (kN) fairlead 1	-931.9	-1492.4	-1669.9	-919.9	-1495.5	-1659.3
Maximum Tz (kN) fairlead 2	-624.0	-761.7	-893.7	-517.3	-632.0	-749.3
Maximum Tz (kN) fairlead 3	-637.7	-778.8	-899.8	-512.0	-597.4	-710.7

Table 4-20 Maximum offsets, nacelle accelerations, fairlead displacements and loads, ActiveFloat Morro Bay

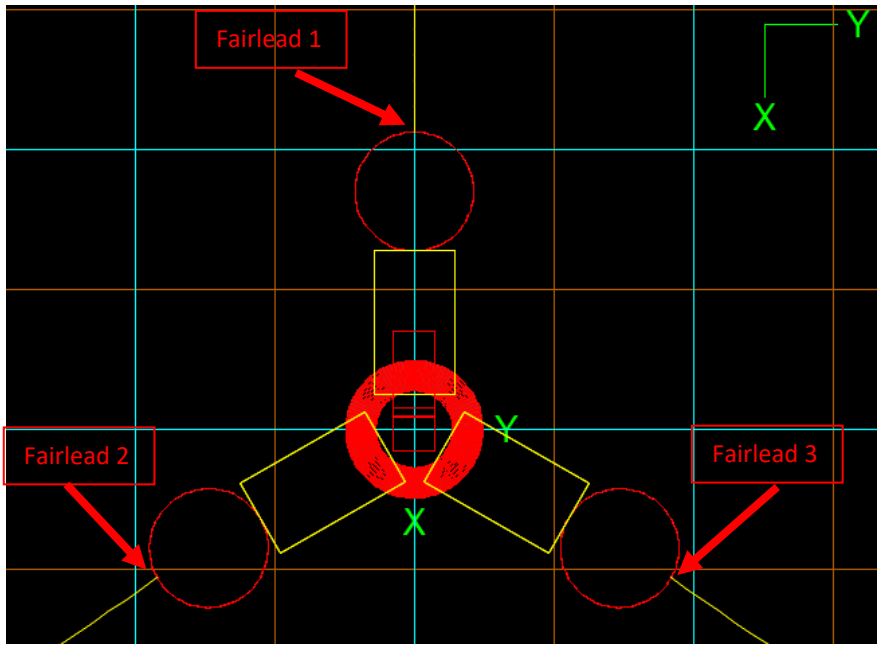

Figure 4-9 Illustration of the location of the three fairleads

Fairlead and connection displacements with respect to their position in the static state are all of similar magnitudes, so that conclusions would not be relevant at this stage.

The loads magnitudes are similar when comparing the mooring system equipped with System 1 and the initially optimized mooring system without PLRS.

To conclude on this part, it has been pointed out that the use of PLR systems attached to the mooring lines conducted to significant load reductions at the fairleads, leading to 50% reduction for both floaters on the site of Gran Canaria. In addition, nacelle accelerations and maximum offset could be reduced when using PLR systems on ActiveFloat's mooring system at the site of Gran Canaria. In the other cases studied, no significant discrepencies have been observed. Therefore, it can be concluded that the use of PLR systems has a positive influence on the fairleads loads and displacements that varies significantly with the type of floater and environmental condition.

4.3 Experimental outcomes on mooring system influence on platforms

This section gives an overview of the mooring system influence on the WindCrete and ActiveFloat platform based on the experimental results. The results are extracted from D5.3 Integrated FOWT test report which summarizes the fully coupled experimental tests conducted in both POLIMI and FIHAC facilities carried out within the framework of Task 5.4.

The mooring systems used for the experiments are the optimized designs truncated to allow the water depth reduction to achieve the desired scale factor. The results presented account for dynamic wind and irregular wave trains with and without current.

4.3.1 WindCrete experimental results

The Figure 4-10 shows the WindCrete experimental reference system and the nomenclature used for the results. The Load Cells placed on the delta connections and on the fairleads have the same number correlated with the nomenclature shown in the figure. For the analysis of the tensions, only the results of the main line 1 will be shown, where the LC1 is the tension of the load cell (LC) at the delta connection 1, the LC4 is the tension of the load cell placed at the fairlead of the delta line 4, and the LC5 is the tension of the load cell at the fairlead of the delta line 5.

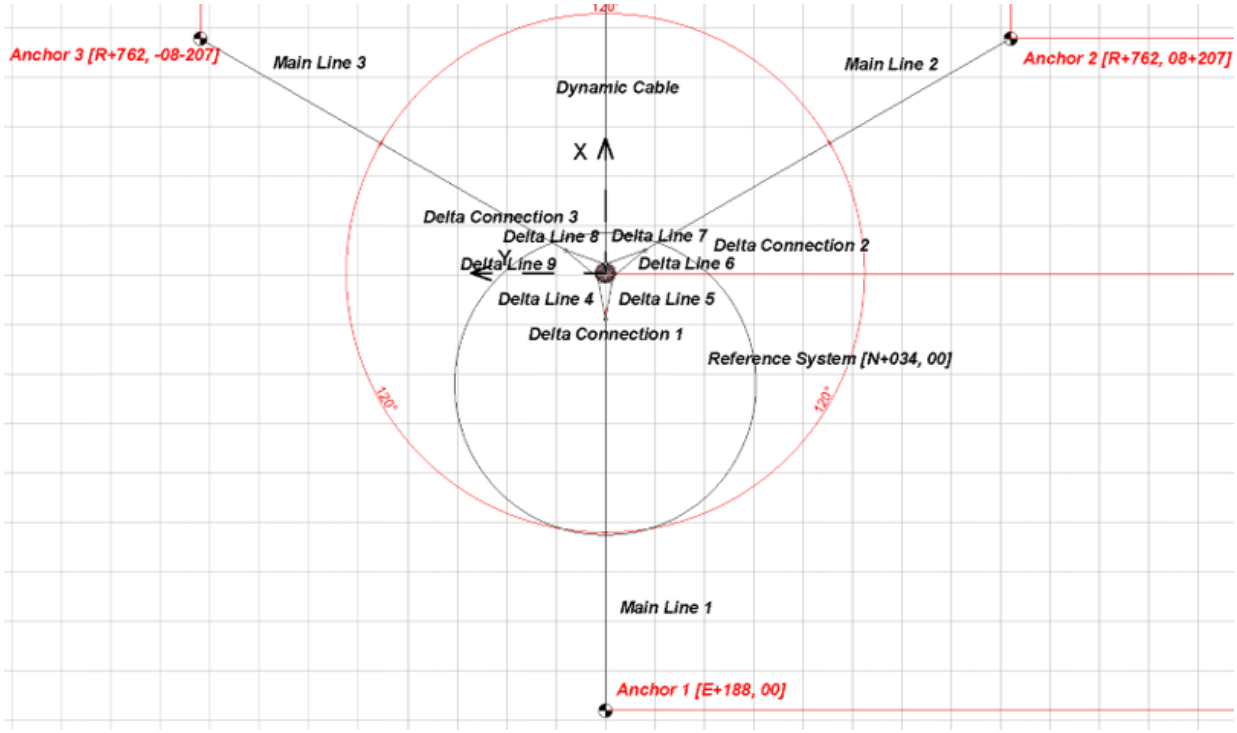

Figure 4-10: WindCrete experimental test reference system and nomenclature

The Table 4-21 and Table 4-22 show the Test analyzed for the WindCrete platform in this section. The test are a combination of dynamic wind at rated wind speed (10.5m/s), under rated wind speed (9 m/s) and over rated wind speed (18m/s), operational sea state (Hs = 2.75m) and severe sea state(Hs = 5.11m) and with and without current of 1.06 m/s.

Configuration WC2 [0 degrees] Irregular Wave + Wind												
Test	Hs [m]		Tp [s]		Spectrum	h [m]	Current [m/s]		Wind [m/s]	Thrust [tonnes]	Direction [º]	Duration [h]
	1/1	1/55	1/1	1/55			1/1	1/55				
52	2.75	0.050	9	1.214	JS-3.3	165	0	0	10.5 ETM	174.26	0	3
53	5.11	0.093	9	1.214	JS-1.2	165	0	0	10.5 NTM	176.71	0	3
54	5.11	0.093	9	1.214	JS-1.2	165	0	0	9 NTM	194.76	0	3
55	5.11	0.093	9	1.214	JS-1.2	165	0	0	18 NTM	92.23	0	3
56	2.75	0.050	9	1.214	JS-3.3 s = 6	165	0	0	10.5 ETM	175.29	0	3
57	2.75	0.050	9	1.214	JS-3.3 s = 12	165	0	0	10.5 ETM	175.21	0	3

Table 4-21. Configuration WC2: Irregular wave and Wind tests. All values are presented at full scale, except for the significant wave heights, wave peak periods and current velocities which are also presented at model scale

Configuration WC2 [0 degrees] Irregular Wave + Current + Wind												
Test	Hs [m]		Tp [s]		Spectrum	h [m]	Current [m/s]		Wind [m/s]	Thrust [tonnes]	Direction [º]	Duration [h]
	1/1	1/55	1/1	1/55			1/1	1/55				
59	2.75	0.050	9	1.214	JS-1.0	165	1.06	0.143	10.5 ETM	174.99	0	3
60	5.11	0.093	9	1.214	JS-1.2	165	1.06	0.143	10.5 NTM	193.88	0	3

Table 4-22. Configuration WC2: Irregular wave, Current and Wind tests. All values are presented at full scale, except for the significant wave heights, wave peak periods and current velocities which are also presented at model scale

- **Wave and wind**

Table 4-23 reports the mean, and maximum absolute values of the platform 6DOF motions at the MSL Position. Table 4-24 and Table 4-25 reports the mean, minimum and maximum values of the acceleration and tensions of mooring line 1 for the main line (LC1) and for the delta lines (LC4 and LC5).

The motion results shows a maximum mean pitch and a maximum absolute pitch of 4.17 degrees and 6.51 degrees respectively.

#	Motion											
	X [m]		Y [m]		Z [m]		roll [deg]		pitch [deg]		yaw [deg]	
	mean	max	mean	max	mean	max	mean	max	mean	max	mean	max
52	7.07	12.74	0.49	1.01	-1.86	2.65	0.45	0.69	3.76	6.43	1.04	1.32
53	7.32	11.95	0.51	1.13	-1.86	2.86	0.45	0.76	3.84	6.17	1.04	1.3
54	8.09	11.87	0.46	0.87	-1.88	2.83	0.47	0.68	4.17	6.2	1.04	1.32
55	3.83	7.41	0.7	1.13	-1.73	2.69	0.34	0.56	2.34	4.56	1.08	1.28
56	7.24	12.66	0.5	1.08	-1.84	2.74	0.44	0.76	3.78	6.41	1.09	1.41
57	7.21	12.82	0.5	1.05	-1.89	2.77	0.45	0.79	3.8	6.51	1.07	1.41

Table 4-23. Configuration WC2: Combined Irregular Wave and Wind. Motions results in the MSL Position

The accelerations results show values under the operational limits with a maximum of 1.52 m/s^2.

#	Accelerations - Nacelle [m/s^2]					
	Acc. X		Acc. Y		Acc. Z	
	max	min	max	min	max	min
52	0.83	-0.74	0.10	-0.10	0.06	-0.08
53	1.52	-1.37	0.22	-0.29	0.10	-0.13
54	1.51	-1.34	0.19	-0.19	0.09	-0.15
55	1.47	-1.39	0.19	-0.19	0.10	-0.13
56	0.75	-0.67	0.29	-0.28	0.08	-0.07
57	0.82	-0.80	0.35	-0.30	0.08	-0.07

Table 4-24. Configuration WC2: Combined Irregular Wave and Wind. Accelerations results in the Nacelle Position

The maximum tension in the main line 1 equal to 663 tonnes whereas the maximum tension of the delta line is equal to 333 tonnes.

#	Mooring Line 1 - Load [tonnes]								
	LC1			LC4			LC5		
	mean	max	min	mean	max	min	mean	max	min
52	426.29	662.70	299.80	212.57	329.93	152.98	215.58	333.31	150.91
53	433.52	572.99	318.21	215.93	283.95	161.44	218.86	289.85	160.02
54	448.20	584.63	335.74	223.29	291.80	167.92	226.15	293.36	170.74
55	370.66	484.34	292.83	184.62	240.40	147.57	188.44	245.20	150.00
56	428.44	649.66	303.94	212.42	326.02	152.57	217.17	324.37	153.43
57	429.57	660.58	303.60	213.37	330.40	153.61	217.08	329.99	150.49

Table 4-25. Configuration WC2: Combined Irregular Wave and Wind. Mooring system results: Line 1

- **Wave, Wind and current**

Table 4-26 reports the mean, and maximum absolute values of the platform 6DOF motions at the MSL Position. Table 4-27 and Table 4-27 reports the mean, minimum and maximum values of the acceleration and tensions of mooring line 1 for the main line (LC1) and for the delta lines (LC4 and LC5).

The motion results shows a maximum mean pitch and a maximum absolute pitch of 4.39 degrees and 6.74 degrees respectively which are almost the same values than the results without current.

#	Motions											
	X [m]		Y [m]		Z [m]		roll [deg]		pitch [deg]		yaw [deg]	
	mean	max	mean	max	mean	max	mean	max	mean	max	mean	max
59	7.42	13.06	1.62	11.75	-2.03	2.92	0.4	1.5	3.94	6.74	1.06	1.65
60	8.29	12.34	1.38	10.68	-2.06	3.07	0.45	1.64	4.39	6.34	1.07	1.63

Table 4-26: Configuration WC2: Combined Irregular Wave and Current and Wind. Motions results in the MSL Position

The accelerations results show values under the operational limits with a maximum of 1.74 m/s^2.

#	Accelerations - Nacelle [m/s^2]					
	Acc. X		Acc. Y		Acc. Z	
	max	min	max	min	max	min
59	0.98	-0.90	0.52	-0.52	0.08	-0.08
60	1.74	-1.48	0.70	-0.65	0.14	-0.15

Table 4-27. Configuration WC2: Combined Irregular Wave and Current and Wind. Accelerations results in the Nacelle Position

The maximum tension in the main line 1 is 816 tonnes whereas the maximum tension of the delta line is 448 tonnes. An increase of the mooring tensions of 23% for the main line and of 35% for the delta line with respect the experimental results without current can be identified.

#	Mooring Line 1 - Load [tonnes]								
	LC1			LC4			LC5		
	mean	max	min	mean	max	min	mean	max	min
59	539.79	800.37	379.68	288.38	446.06	204.59	259.10	395.66	182.06
60	561.06	815.77	423.74	300.44	447.82	227.43	260.54	385.95	194.61

Table 4-28. Configuration WC2: Combined Irregular Wave and Current and Wind. Mooring system results: Line 1

4.3.2 ActiveFloat results

The Figure 4-11 shows the ActiveFloat experimental reference system and the nomenclature used for the results. The Load Cells placed on the fairleads have the same number correlated with the nomenclature shown in the figure.

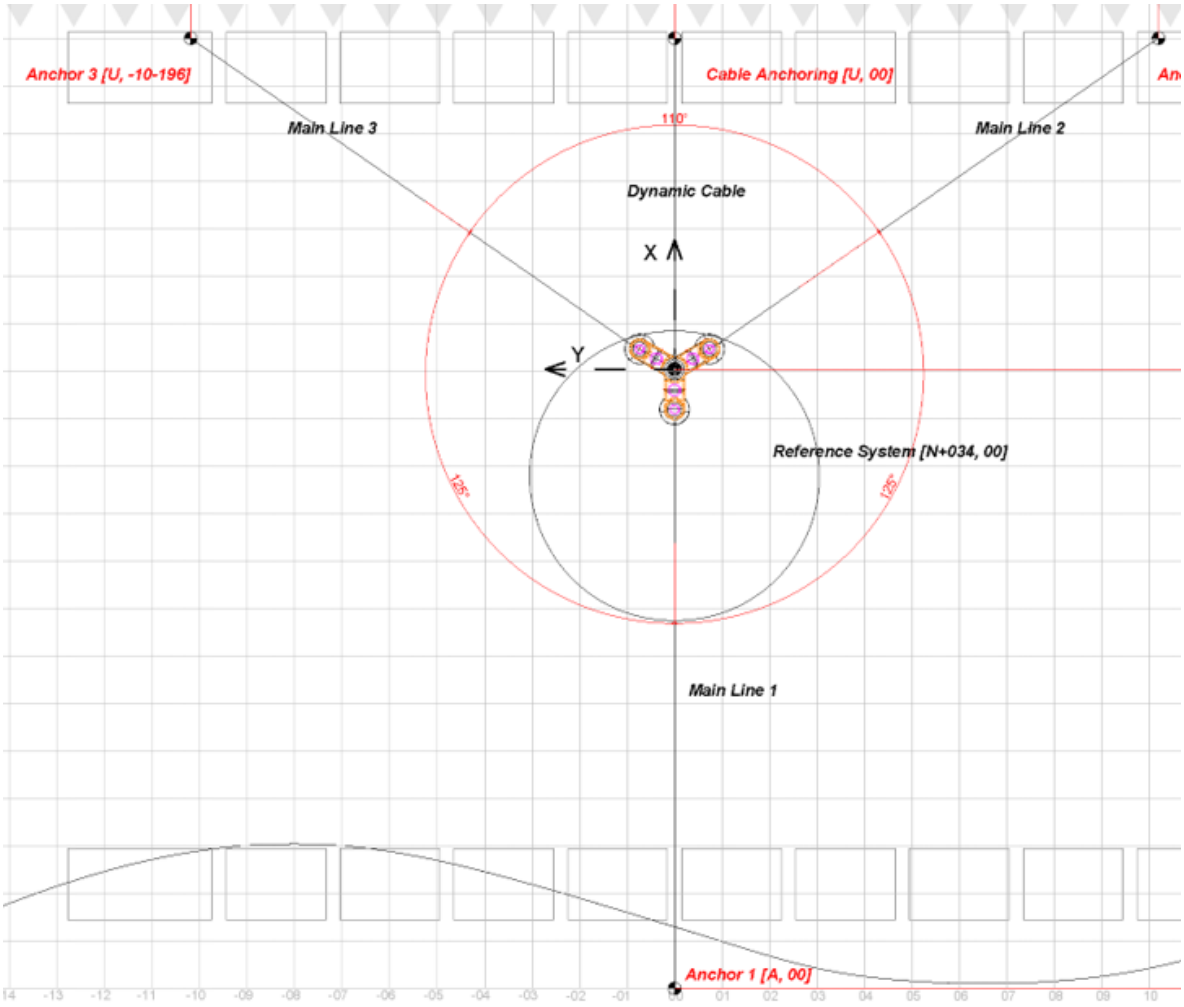

Figure 4-11: ActiveFloat experimental test reference system and nomenclature

- **Wave and wind**

The Table 4-29 and Table 4-30 show the Test analyzed for the Active platform in this section. The tests are a combination of dynamic wind at rated wind speed (10.5m/s), operational sea state (Hs = 2.75m) and severe sea state(Hs = 5.11m) and with and without current of 1.06 m/s.

Configuration AF3 [0 degrees] Irregular Wave + Wind												
Test	Hs [m]		Tp [s]		Spectrum	h [m]	Current [m/s]		Wind [m/s]	Thrust [tonnes]	Direction [º]	Duration [h]
	1/1	1/40	1/1	1/40			1/1	1/40				
112	2.75	0.069	9	1.423	JS-3.3	120	0	0	10.5 ETM	173.58	0	3
113	5.11	0.128	9	1.423	JS-1.2	120	0	0	10.5 NTM	193.29	0	3
114	2.75	0.069	9	1.423	JS-3.3 s = 6	120	0	0	10.5 ETM	173.29	0	3
115	2.75	0.069	9	1.423	JS-3.3 s = 12	120	0	0	10.5 ETM	174.02	0	3

Table 4-29. Configuration AF3: Irregular wave and Wind tests. All values are presented at full scale, except for the significant wave heights, wave peak periods and current velocities which are also presented at model scale

Configuration AF3 [0 degrees] Irregular Wave + Current + Wind												
Test	Hs [m]		Tp [s]		Spectrum	h [m]	Current [m/s]		Wind [m/s]	Thrust [tonnes]	Direction [º]	Duration [h]
	1/1	1/40	1/1	1/40			1/1	1/40				
117	2.75	0.069	9	1.423	JS-1.0	120	1.06	0.168	10.5 ETM	173.99	0	3
118	5.11	0.128	9	1.423	JS-1.2	120	1.06	0.168	10.5 NTM	193.63	0	3

Table 4-30. Configuration AF3: Irregular wave, Current and Wind tests. All values are presented at full scale, except for the significant wave heights, wave peak periods and current velocities which are also presented at model scale

- **Wave and wind**

Table 4-31 reports the mean, and maximum absolute values of the platform 6DOF motions at the MSL Position. Table 4-32 and Table 4-33 report the mean, minimum and maximum values of the acceleration and mooring line tensions for the main lines 1, 2 and 3 (LC1, LC2 and LC3).

The motion results show a maximum mean pitch and a maximum absolute pitch of -1.94 degrees and 8.01 degrees respectively. The surge excursion has a maximum value of 43.5m.

	Motions											
	X [m]		Y [m]		Z [m]		roll [deg]		pitch [deg]		yaw [deg]	
	mean	max	mean	max	mean	max	mean	max	mean	max	mean	max
112	29.8	43.31	-0.24	1.5	0.35	0.97	0.48	0.69	-1.92	7.69	0.93	2.96
113	33.92	41.34	0.49	2.6	2.6	1.44	0.49	0.84	-1.28	5.21	1.04	2.43
114	29.69	43.45	-0.25	3.47	2.46	1.01	0.46	0.96	-1.94	8.01	0.91	4.24
115	29.72	43.5	-0.12	3.05	2.19	0.85	0.46	0.86	-1.93	7.86	0.89	3.95

Table 4-31. Configuration AF3: Combined Irregular Wave and Wind. Motions results in the MSL Position

The accelerations results show values under the operational limits with a maximum of 1.10 m/s^2.

#	Accelerations - Nacelle [m/s2]					
	Acc. X		Acc. Y		Acc. Z	
	max	min	max	min	max	min
112	0.97	-0.62	0.13	-0.08	0.2	-0.27
113	0.78	-0.8	0.17	-0.16	0.33	-0.46
114	0.89	-0.63	0.25	-0.22	0.22	-0.31
115	1.1	-0.59	0.21	-0.22	0.15	-0.29

Table 4-32. Configuration AF3: Combined Irregular Wave and Wind. Accelerations results in the Nacelle Position

The maximum tension in the main line 1 is 449 tonnes.

#	Mooring Line 1 - Load [tonnes]								
	LC1			LC4			LC5		
	mean	max	min	mean	max	min	mean	max	min
112	230.32	444.82	109.82	34.44	46	30.15	35.47	47.03	29.77
113	267.51	428.87	149.15	33.16	38.98	29.76	33.36	40.79	29.21
114	228.45	449.31	111.15	34.47	46.68	29.83	35.6	47.04	29.27
115	227.92	439.37	104.56	34.48	47.74	30.11	35.43	47.47	29.53

Table 4-33. Configuration WC2: Combined Irregular Wave and Wind. Mooring system results

- **Wave, Wind and current**

Table 4-34 reports the mean, and maximum absolute values of the platform 6DOF motions at the MSL Position. Table 4-35 and Table 4-36 report the mean, minimum and maximum values of the acceleration and mooring line tensions for the main lines 1, 2 and 3 (LC1, LC2 and LC3).

The motion results show a maximum mean pitch and a maximum absolute pitch of -2.12 degrees and 8.03 degrees respectively which are almost the same values than the results without current. The surge excursion has a maximum value of 46.9m. Also, the maximum yaw motion presents a large rotation of 12.5 degrees.

#	Motions											
	X [m]		Y [m]		Z [m]		roll [deg]		pitch [deg]		yaw [deg]	
	mean	max	mean	max	mean	max	mean	max	mean	max	mean	max
117	35.88	43.11	1.87	18.64	0.27	0.86	0.53	0.99	-2.12	8.03	1.44	12.53
118	39.27	46.94	3.27	21.97	21.97	1.84	0.54	1.28	-1.45	5.43	1.22	9.87

Table 4-34: Configuration AF3: Combined Irregular Wave and Current and Wind. Motions results in the MSL Position

The accelerations results show values under the operational limits with a maximum of 0.93 m/s^2.

#	Accelerations - Nacelle [m/s2]					
	Acc. X		Acc. Y		Acc. Z	
	max	min	max	min	max	min
117	0.89	-0.62	0.39	-0.3	0.22	-0.25
118	0.93	-0.77	0.5	-0.41	0.45	-0.58

Table 4-35. Configuration AF3: Combined Irregular Wave and Current and Wind. Accelerations results in the Nacelle Position

The maximum tension in the main line 1 is 540.6 tonnes. An increase of the mooring line tension of 20% for the main line 1 with respect the experimental results without current can be seen.

#	Mooring Line 1 - Load [tonnes]								
	LC1			LC4			LC5		
	mean	max	min	mean	max	min	mean	max	min
59	298.99	455.87	196.68	34.8	57.1	25.48	33.59	51.34	24.9
60	349.89	540.59	246.26	34.45	59.67	24.83	32.06	46.27	23.03

Table 4-36. Configuration AF3: Combined Irregular Wave and Current and Wind. Mooring system results

5 Influence of Cabling System on Floater Response and Global Loads

5.1 Cable loading effect on the platform

Maximum tension in the cabling system has been shown to occur at the cable exit from the platform as shown in Corewind Deliverable 3.2 [5]. Maximum tension in the cable system is identified to with the platform in its furthest offset condition, under normal and extreme design limit environmental conditions. It has been shown that the cable load has a negligible effect on platform movement. This is demonstrated both by WP3 modelling results (see D3.2), and by prototype testing where observers concluded that the cable system attached to the moored platform had a negligible influence on the moored platform motion when the system was subjected to environmental loading (see D5.3). Although in normal operation tensions may not influence platform motion, it is recommended that mooring line system design (which limits platform excursions and local motion) be linked to cable system design. With greater offsets relative to water depth, and greater local motion, greater challenges are posed for the cable system development and greater risks to in place design life (see D3.3). Therefore the allowable offsets and platform motion targets for the mooring platform system design should be developed in conjunction/with consideration to cable system design to ensure LCOE is as low as possible across the wind farm systems.

The structural design of the cable exit point from the structure is critical to ensuring a robust connection. This connection is critical as without the cabling system, no power generated by the turbine can be transported to shore for use. Figure 5-1 illustrates two industry options for J-tube/I-tube exit design; 1) fixed connections with purpose built cable bend protection (such as a Bend stiffener), or 2) adapting the tube exit to a bellmouth flared shape to offer only a curvature path guidance to the cable at the exit point.

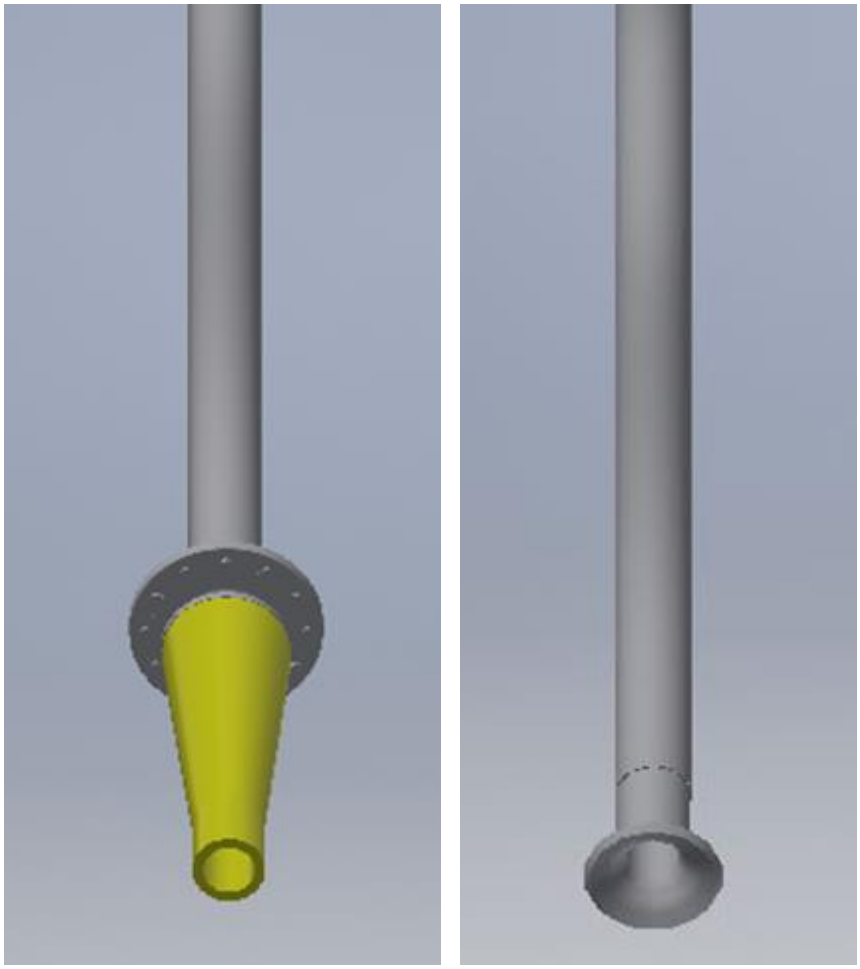

Figure 5-1: Cable exit of J-tube structure: Cable Bend protection (left) vs Bellmouth (right)

A bellmouth design is advantageous for installation purposes, as cables are simpler and quicker to install as it allow more flexibility on approach. For moored platforms with fairly restricted offsets and sufficient water depths (e.g. <15% water depth sized offsets in 150-250 m) with mild operational environmental conditions at cable platform exit point and on the cable system within the water column, a bellmouth may be a viable option. Based on modelling carried out within the Corewind project, with platform exits 10m below the pontoon, to avoid cable extreme limit violations and mitigate excessive fatigue within the cabling system, for all sites the platform exit of the structure required a fixed J-tube with a latch mechanism and bend protection to be employed. As site B in particular is expected to represent typical floating offshore windfarm conditions, it's expected most windfarms will require this arrangement in the near future.

Cable system modelling should inform exit angles of the J-tube to avoid unnecessary loading on the cable and structure, with consideration to avoid clashing of the cable with the platform structure and nearby lines (see D3.3 for further guidance). Unnecessary loading can lead to over-engineering structure solutions, or impose creep into cable bend protectors at this exit point (see D3.3 for bending protector design guidance). The solution should take into account the worst loading seen across both start of life (installed product) and end of life (end of service life condition with build-up of marine growth and loss of buoyancy in buoyancy modules). Maximum bending moment and shear forces should be taken into account during design of the I-tube/J-tube cable exit. This is only possible to

provide with confidence once the bending protection has been designed and applied into the system to predict accurate loading conditions.

No limits were defined by participants for cable system platform exit or interface loading within Corewind, however bending moment and shear force were minimised where possible. Cable system results seen within Corewind modelling are presented in Table 5-1 for site B at Grand Canaria, to provide examples of expected structure loading conditions for further design. It was noted, for the 'optimised' systems the forces were generally greater than the initial modelling due to reductions in cable hardware requirements (e.g. reduction in buoyancy modules) driven by LCOE targets across a large windfarm, and relaxations on the mooring system leading to changes in platform motion. There is a direct correlation between system configuration (including hardware such as buoyancy limits) and loading imparted to the platform structure at the cable exit, so for smaller scale projects with longer cable system target design life, it may be preferable to reduce loading at this connection point from a structural design and cable loading perspective, and adjust cabling system hardware accordingly to lower fatigue imparted near the structure exit point. Where this is likely, structural loading targets should be provided to cable system developers in advance. Where structural loading is not yet know for a system (early stages), based on the results in Corewind it appears reasonable to assume maximum allowable tensile loading of the cable at the exit point, until more detailed information is available from detailed cable system modelling.

Table 5-1: Gran Canrtia - Forces at Cable exit under extreme loading conditions

Parameter	Results
Maximum Effective Tension (kN)	155.11
Mean Bending Moment (kNm)	0.35
Mean Shear Force (kN)	0.11

For fatigue consideration of the cable, a design fatigue factor (DFF) should be selected to cover uncertainties when assessing loads onto structures and for variations in material properties, and any safety related ramifications of failure. Location and risk should be carefully considered for design of structures throughout the floating windfarm, which will be greater than the risk on a static windfarm. CIGRE 862, with reference to DNV-ST-0119, identifies DFF classifications for structure design in mooring lines and dynamic cables (see D3.3 for further details). As a baseline for the entrance structure, DNV-ST-0145 indicates that J-tubes should be designed to meeting high safety classification, and subsequently a DFF of 10 is recommended for the industry.

Consideration should also be given to the structure design for the cabling system from a thermal perspective. This includes evaluations on size, thickness and surface absorptivity of solar radiation when designing the cable tube on the outer portion of the structure, particularly where exposed to direct sunlight. can limit the maximum current carried by a cable within the structure, and therefore feed directly into cable and structure design. The adoption of common static windfarm yellow coating is recommended to be adopted for floating wind to ensure minimal absorptivity, and thus reduced ramifications to thermal design, as well as retain high visibility of the structure.

5.2 Influence of the cable routing and connection considerations for platform structure design

As advised in CIGRE 862, there are two types of cable disconnection that may be necessary for the connection within the platform structure to facilitate; accidental disconnection and planned disconnection.

In planned disconnection events, the cable is carefully detached from the rest of the platform and ends are sealed to prevent water ingress. Where more than one disconnection is planned during service life, industry models currently consider disengaging the connection within the structure, and having the J-tube section of the structure able to separate from the main structure. The advantage of this system is that the bulk of the cable remains in place and intact, and reattachment is relatively straight forward. The separated structure needs to be controlled to avoid excessive offset from the original position (e.g. tethered to the seabed). Given this smaller structure is often less stable than the main platform structure under environmental loading, more erratic movement is often induced in the cable under this scenario, and subsequently the fatigue induced to the cable under this arrangement will typically be greater than when the cable system is attached to the full platform. Control and modelling of this disconnected case is extremely important if this method of disengagement is planned during service.

Of primary importance in platform structure design is accidental disconnections for the cable system, also commonly referred to as “weak link” connection systems. This is designed to activate during accidental events. This is required even when no planned disconnections are expected during the life of the cabling system. An accidental disconnection is a consideration where the cable system exceeds its design limits. An example of this is the loss of an anchor or mooring line, where the structure may drift further than the cable system is designed to tolerate, and subsequently higher tensions and bending loads would be seen at the cable exit of the structure. This would damage the cable system at this end, but more importantly load the structure to a degree it was not designed to tolerate, leading to damage and potentially unwanted pivoting effects about this point. Mitigation to limit damage in these accidental cases is employed by designing a cable emergency disconnection system within the structure, typically triggered by excessive tensions, so the cable releases prior to excessive loading on the main platform structure.

Given the cable engagement within the structure, there are 3 parts to any emergency disconnection system. As shown in Figure 5-2, this consists of:

1. Disconnection of the cable at the cable entrance point, typically where the bend restrictor is located.
2. Disconnection of the cable at the hang off point in the structure (i.e. where the cable strength members are terminated)
3. Disconnection of the cable’s power cores are terminated/jointed to the main platform circuitry.

These 3 disconnections must be triggered in conjunction (i.e. immediate succession) to ensure the cable disconnects from the structure smoothly. The structure design must facilitate this disconnection to ensure the cable disconnection hardware does not get jammed in the J-tube.

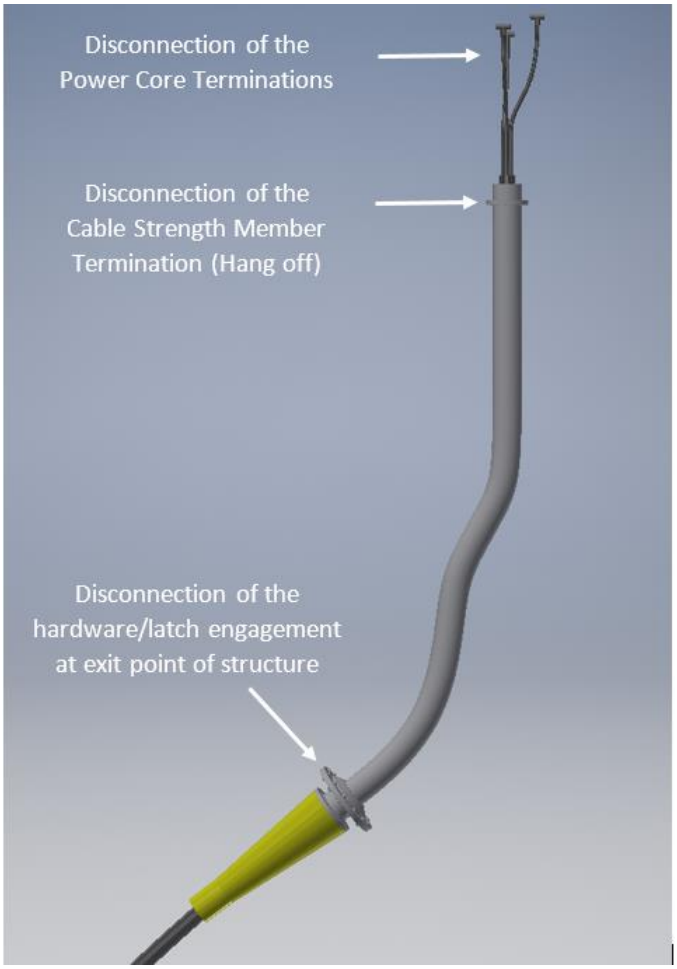

Figure 5-2: Location of disconnection points within accidental disconnection system

Although it is expected the disconnection will be predicted prior to disconnection event (due to O&M strategies detecting loss of the mooring line for example), H&S is of paramount importance when considering the structure design. This accidental disconnection should minimise damage to the surrounding structures.

To limit the risk to this smooth disconnection, it is advisable to have points 2 and 3 as close as possible to each other and directly in line with point 1 where possible. Where there is a significant route to travel between the hang off and the WTG termination, particularly if this is routed out of line of the hang off, it is strongly recommended a jumper cable is used so that the disconnection unit can be separated to mitigate risks to the disconnection process.

Accurate platform behaviour modelling when designing the cable system is essential to the design of the cable's accidental disconnection system. If platform movement does not capture extremes of the platform motion expected, the accidental disconnection system may be triggered unintentionally during normal operating conditions. If the triggering tension window identified (if this is the method employed) is set too high, this may endanger the platform and increase costs to structure design around the 3 levels of cable engagement (outlined above). Consideration for this triggering window should be given to disconnection method chosen and system sensitivities, often limited by material tolerances.

6 Design Recommendations for Connection of Moorings to Concrete Floaters

6.1 Introduction

The structural elements affected by the mooring system represent key elements for achieving the desired structural robustness of a floating wind platform.

6.2 Mooring Connection Design overview

6.2.1 Fairleads

The fairlead connections will be typically located at the outer face of the hull. The connection of the mooring line is done firstly to the fairlead that is welded to a base plate, which in turn is anchored to the wall or to the top of the hull.

Thus, the fairlead is a system which connects the mooring line to the hull by means of an anchored base plate. Fairleads are usually formed by one or two hinges that allow the rotations in vertical and horizontal axis in order to reduce the moments on the base plate.

The Figure 6-1shows a typical fairlead that allows vertical and horizontal rotations, and a base plate which is connected to the hull by means of anchor bolts. In this case the fairlead is built by two horizontal padeyes which allow the double vertical padeye to rotate horizontally. This double vertical padeye allows the mooring to rotate vertically by means of an intermediate pin.

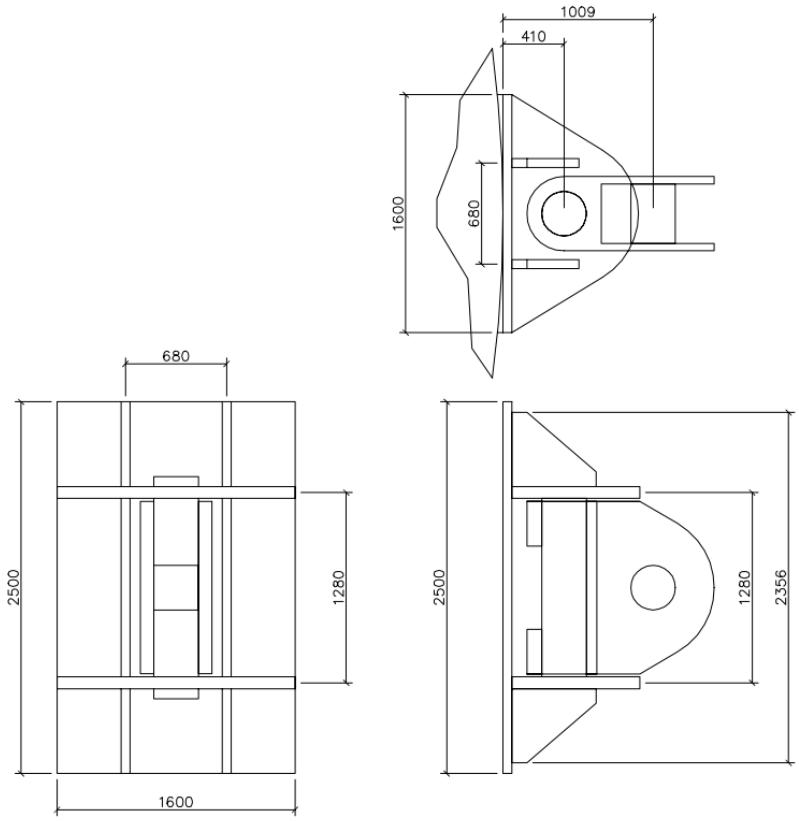

Figure 6-1 – Fairlead proposed for Activefloat. General arrangement

A key factor on the design of the mooring connections is the distance of the hinges to the base plate, which will define the eccentricities of the mooring forces and, therefore, the moments that influence the design, as shown in Figure 6-2.

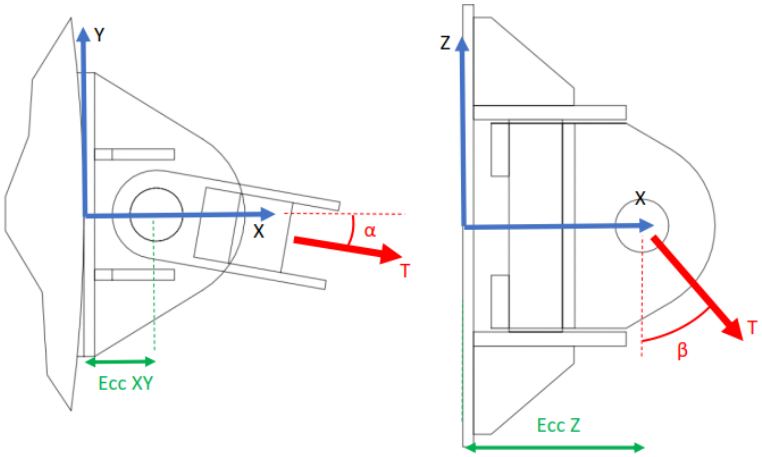

Figure 6-2 – Free rotations and eccentricities of the fairlead proposed for Activefloat.

6.2.2 Base Plate

The base plate connects the fairlead itself to the hull. The dimensions and thickness of the base plate depend on the fairlead and on the hull structures. In the case of a steel hull the transmission of forces coming from the fairlead steel plates may be done directly to an internal bulkhead or other transverse reinforced girder. However in the case of a concrete hull, the forces coming from the fairlead plates need to be spread by means of the base plate. The use of stiffeners will allow to reduce the thickness of the base plate but will also reduce the space to place the anchor bolts (Figure 6-3).

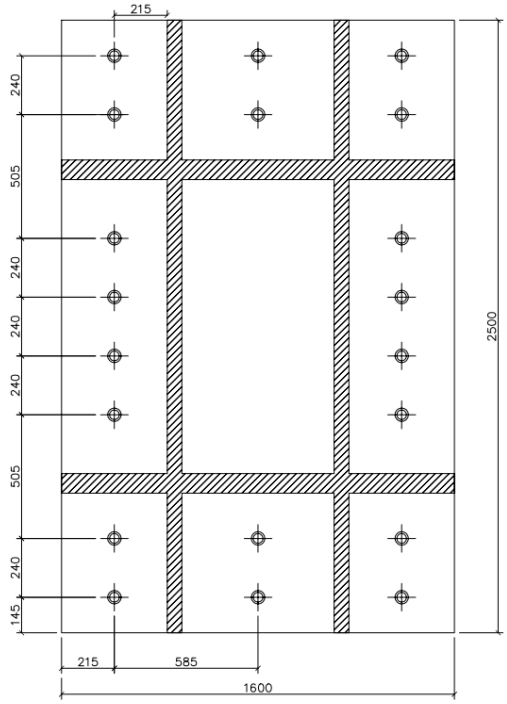

Figure 6-3 - Base plate of the fairlead connection proposed for Activefloat.

6.2.3 Anchor bolts

The connection of the base plate to a concrete hull may be done by means of anchor bolts or threaded bars, bounded or unbounded.

In order to limit the fatigue in the anchor bolts and have a good performance of the connection, they must be post-tensioned. The compression applied should be sufficient to prevent decompression in the contact between the base plate and the concrete hull under the relevant loads (maximum fatigue load or maximum characteristic extreme load). As long as the contact between base plate and concrete is under compression, the stress ranges of the anchor bolts will be small and the fatigue behaviour of the anchor bolts will be optimal. Nevertheless, the fatigue capacity of the concrete is lower as the compressive stress rises, therefore both the dimensions of the plate and the resistance of the concrete must be consistent.

Special care for the corrosion control and watertightness of the anchorages should be taken. In addition, notice that as these steel bolts or rebars will be in contact with the base plate, which in turns may have a cathodic protection system if it is below HAT. Therefore there is risk of hydrogen embrittlement of the anchor bolts (Hydrogen Induced Stress Cracking). In this case (fairlead below HAT), the bolt class should not exceed ISO 898-1 Class 8.8 (refer to DNV-ST-0119 [7.1.9.1] and DNV-ST-0126 [4.2.6.2]).

6.2.4 Shear Lugs and Headed studs

Transverse forces on the base plate are transferred by friction. However it may be necessary to increase the transverse capacity at ultimate limit state by means of headed studs or shear lugs.

A shear lug consist of an embedded plate in the concrete wall, welded to the base plate, which transfers shear forces by means of a lateral compression loads to the concrete (Figure 6-4).

Another alternative may be to arrange headed stud connectors. They are typically used in composite structures such as bridges to transfer shear loads between steel and concrete. The headed studs are embedded in the concrete wall and welded to the base plate (Figure 6-5).

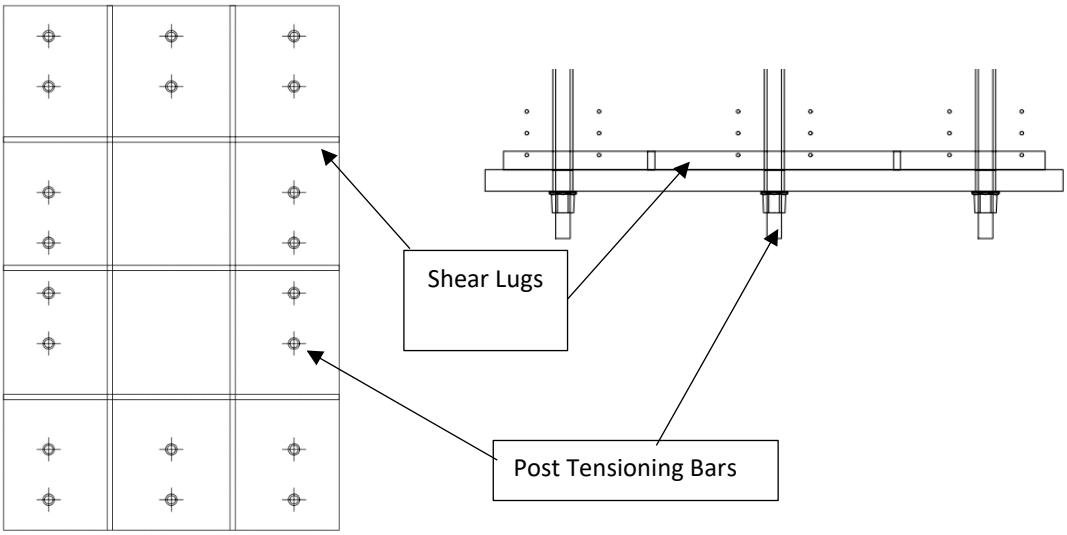

Figure 6-4 – Example of shear lugs welded to the base plate (left: front view; right: side view).

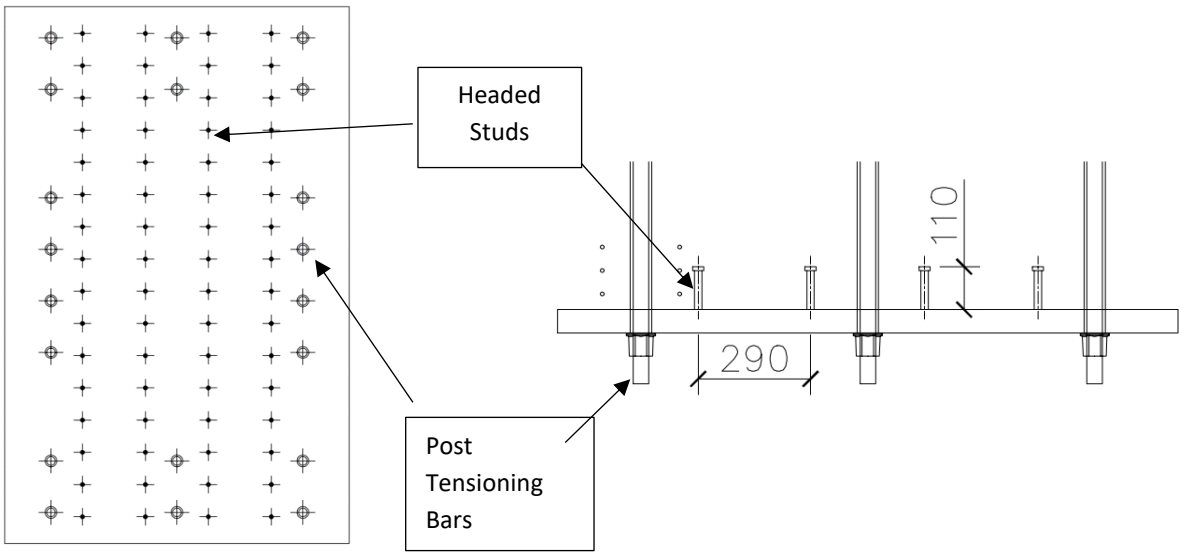

Figure 6-5 – Example of headed studs welded to the base plate (left: front view; right: side view).

6.3 Design recommendations

6.3.1 Design basis

The design of the mooring anchorage may be based on DNVGL-ST-0119 which provides specific requirements for this type of structures, in particular special provisions for concrete structures. Additionally, the structural design code for concrete may be DNVGL-ST-C502 or EN-1992 series.

The minimum design assessment, which is explained in more detail in the next sections, is summarized here below:

- Design loads should be based on the capacity of the mooring or alternatively assessed based on the design loads obtained by the hydrodynamic simulations, including the ALS conditions.
- Anchor bolts and their post-tensioned force should be designed so that there is no decompression under the base plate for the characteristic extreme load combination.
- The ultimate capacity of the anchor bolts shall be verified under the ULS and the ALS combinations.
- A final fatigue assessment of the anchor bolts, reinforcement and concrete shall be carried out.
- Watertight and cracking limits of the concrete shall be controlled.

6.3.2 Design loads

The mooring connections should be designed with sufficient margin to be able to absorb variations in the extreme design loads along the design process, due to natural refinement along the course of design due to, for example, design evolution, analysis and tank testing.

In some types of structures, these types of connections are designed to withstand the breaking load of the connected elements (e.g., cables, tendons or moorings), due to the following reasons:

- Often the structural integrity depends on the integrity of these elements.

- These elements are very difficult to repair or replace.
- Normally, designing these elements to be more robust will not lead to significant global cost increases.

In the same sense, DNV-ST-0119 [7.1.9.1] specifies the characteristic capacity of mooring lines (Sc= 0.95·MBL) as the design load. However, as indicated also in DNV-ST-0119 [7.1.9.1], designing these elements to resist a force close to the minimum breaking load of the connected lines might be excessively conservative in the case of offshore platforms because the design of these lines may be governed by the fatigue assessment and corrosion allowance of the mooring itself. Therefore, the alternative is to design the connection based on the design tension of mooring lines (Td). Nevertheless, notice that DNV-ST-0119 requires some additional DLCs for floating wind turbines, in particular special attention to the DLC 6.6 for ALS robustness check should be paid (500 year of return period for wind or wave loads).

Besides, the components of the tension vector should be taken into account since the anchorage design is very influenced by the direction of the mooring line locally at the anchor point.

6.3.3 Predesign

First step of design should be the dimensioning of the anchor bolts and the minimum dimensions of the base plate so that there is no decompression under the base plate for the characteristic extreme load combination. Long term prestressing forces should be taken into account. The concrete compressive stresses under the base plate shall be limited to 60% of the characteristic compressive strength (0.6 f_{ck}).

Then, anchor bolts shall be verified for ULS and ALS load combinations. The acceptance criteria should be based on DNV-ST-0119 [7.1.9.1]. Notice that for the ALS load combination, the concrete compressive stresses shall be limited to 0.6 f_{ck} and the reinforcement stresses shall be limited to 0.9 $f_{yk??}$ as per DNV-ST-0119 [7.5.2.2].

At this stage, an evaluation of the shear capacity by friction should be carried out to detect the need to have additional elements such as shear lugs or headed studs.

6.3.4 Final design verification

The final design of the mooring connection shall be assess the next:

- Design of local reinforcement at the post-tensioning anchorage areas (bursting and spalling of local zone). Local zone reinforcement may be based on proprietary element detailing specifications or may be designed as partially loaded areas as per EN-1992-1-1 or DNV-ST-C502.

- Design of the general zone strengthening (Figure 6-6) by means of strut-and-tie models which appropriately identify the primary flow of mooring forces from the local zone to the general structural system. The strut-and-tie model should be based on the principal concrete stresses obtained from a 2D or 3D FEM model. Depending on the complexity of the geometry the FEM model may be composed of shell elements or solid elements.

- Minimum reinforcement in accordance with DNV-ST-0119.

- Watertightness and crack width checks in accordance with DNV-ST-0119 and DNV-ST-C502 or EN-1992-1-1 respectively.

- Fatigue assessment of the anchor bolts and reinforcement as per DNV or Eurocodes. Since no decompression should be verified for the maximum fatigue load, equivalent fatigue load or rain-flow-

count spectrum could be used for the anchor bolts, however, the verification should preferably be performed by Markov matrices.

- Fatigue assessment of concrete according to Palmgren Miner's rule as per DNV-ST-C502 or Model Code 2010 and by means of detailed Markov matrices. Greater fatigue damage in concrete are usually just behind the base plate, therefore the stressing force should be controlled to the minimum required as well as a suitable minimum concrete strength should be chosen. Depending on the construction system and sequence, a high strength non-shrink grout may be needed between the base plate and the concrete. This grout also contributes to spread the compression loads to the concrete like in conventional onshore steel tower-foundation connections.

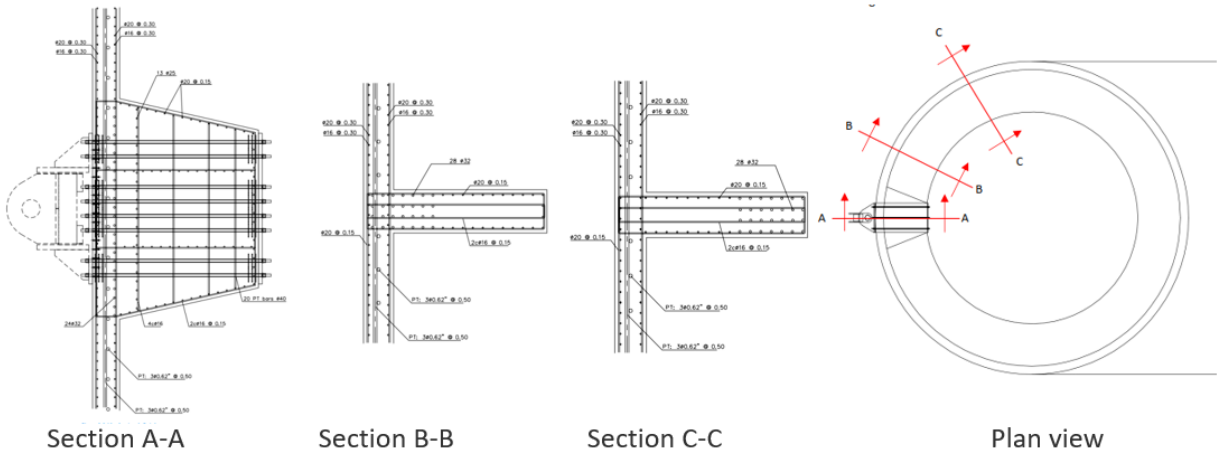

Figure 6-6 Activefloat local strengthening in the fairlead plate anchoring system

6.4 WindCrete connection design particularities

The main particularity of the mooring connection design of the WindCrete concept is the double fairlead at each plate. Thus, the plate have to be larger to allow placing of the two fairleads. Another particularity is the detailed design of the concrete wall at the fairlead zone, which accounts for an increase of the thickness and the need of circumferential tendons to balance the tension forces from the moorings.

- **Double fairlead design**

The mooring connection design presents a double hinge as shown in Figure 6-7 a). This configuration is due to the delta line design to provide the needed yaw stiffness to the system. Then, the plate is designed with a zone free of any post-tensioning bars at the center, where the vertical shafts have to be placed as shown in Figure 6-7 b). This design implies larger mooring loads at the plate mainly in the shear directions, as the mooring lines do not reach the platform in the radial direction. This means that a large number of posttensioning bars are needed in order to balance the bending moment introduced by the tangential forces with eccentricity.

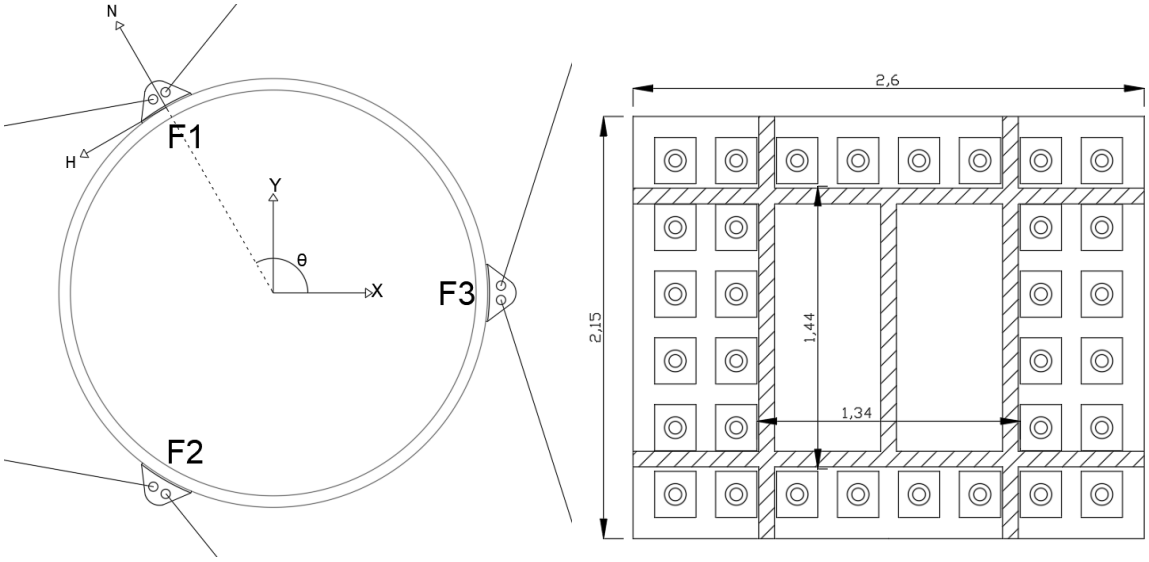

Figure 6-7: WindCrete fairlead connection: a) XY plane view of fairleads global position and orientation. B) Fairlead anchor plate basic scheme (dimensions in m)

- **Detailed design of the concrete wall**

Resultant mooring loads at the fairlead section will produce a tensile stress state due to the tension forces applied. As concrete is not well-suited to resist this kind of stress, circumferential posttensioning tendons will be required in the connection zone. In this case, the circumferential post-tensioning tendons are designed to have two curvatures along the ring. Varying curvature tendons are proposed to reduce local tension effects. The radius of curvature is reduced at points near the fairleads, therefore increasing the equivalent radial centripetal force produced by the prestressing load of the tendon. The radius reduction is achieved by displacing the tendon in the outwards radial direction. Likewise, the radius of curvature is increased at the points of the cylinder circumference which are the furthest away from the fairleads, by displacing the tendon towards the center of the cylinder. The configuration of these tendons was conceived such that there is no interference with the trajectory of any of the longitudinal post-tensioning tendons at any point of the circumference.

Three equidistant points of maximum outwards deviation are located at the fairleads' positions, while three points of maximum inwards deviation are also equidistantly located at the three points in between. The resulting circumferential tendon design can be found in Figure 6-8 with the selected radius of curvature.

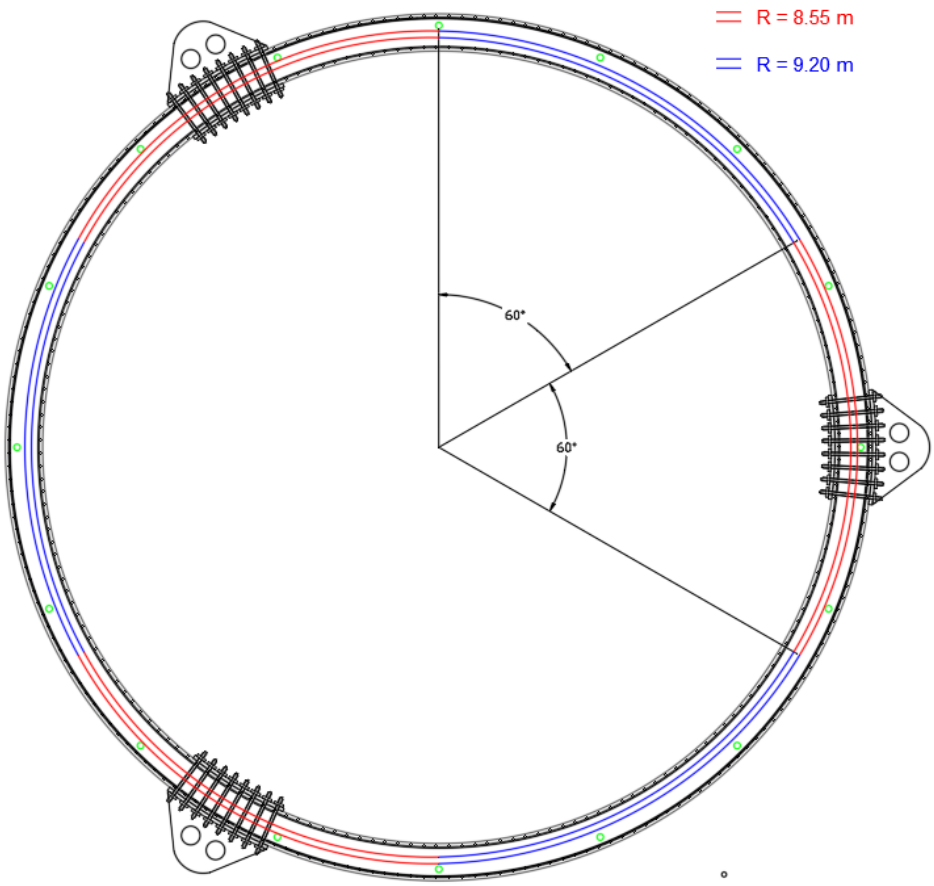

Figure 6-8: Variable curvature, circumferential prestress

Moreover, in order to resist the new compression forces when mooring forces are not acting, an increase of 30 cm of the concrete wall was necessary. The Figure 6-9 shows a drawing of a vertical section at the connection zone. The increase of the thickness of the concrete can be easily seen as well as the distribution of the circumferential tendons.

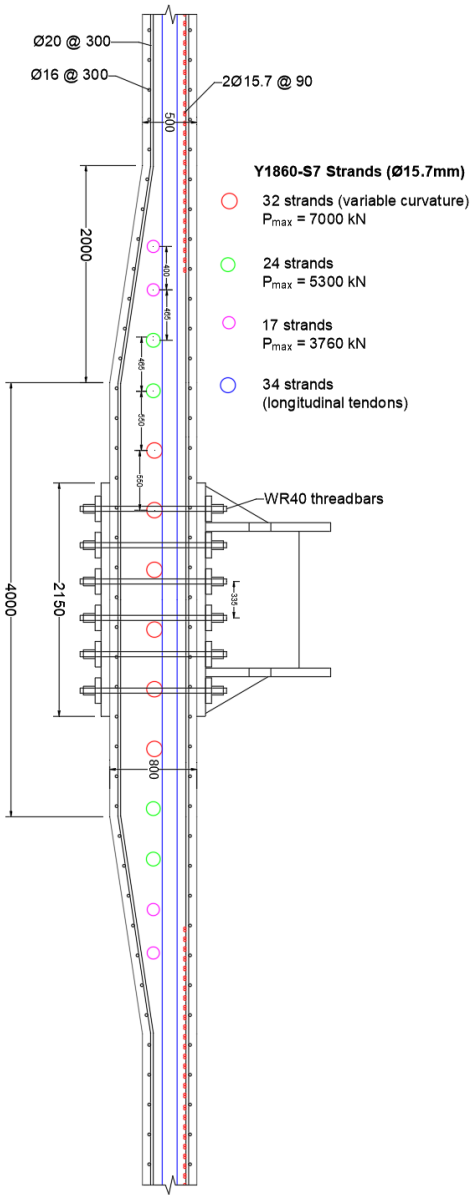

Figure 6-9: WindCrete mooring connection vertical section drawing

6.5 ActiveFloat connection design particularities

One of the major particularities in the ActiveFloat fairlead connection are the necessary internal diaphragm inside the external columns. They are needed so that the mooring forces are transferred in a robust structural element connected to the pontoons and limiting the structural contribution of the columns (see Figure 8.3.2).

As commented in the previous sections, the design of the general zone reinforcement may be carried out by means of strut-and-tie models which appropriately identify the primary flow of mooring forces from the local zone (fairlead connections) to the general structural system (pontoons). The strut-and-tie model should be based on the principal concrete stresses obtained from a 2D or 3D FEM model. Depending on the complexity of the geometry the FEM model may be composed of shell elements or solid elements.

In this particular case, the loads are mainly transferred to the pontoons through the ring stiffener. A strut and tie model was done in order to design the required reinforcement.

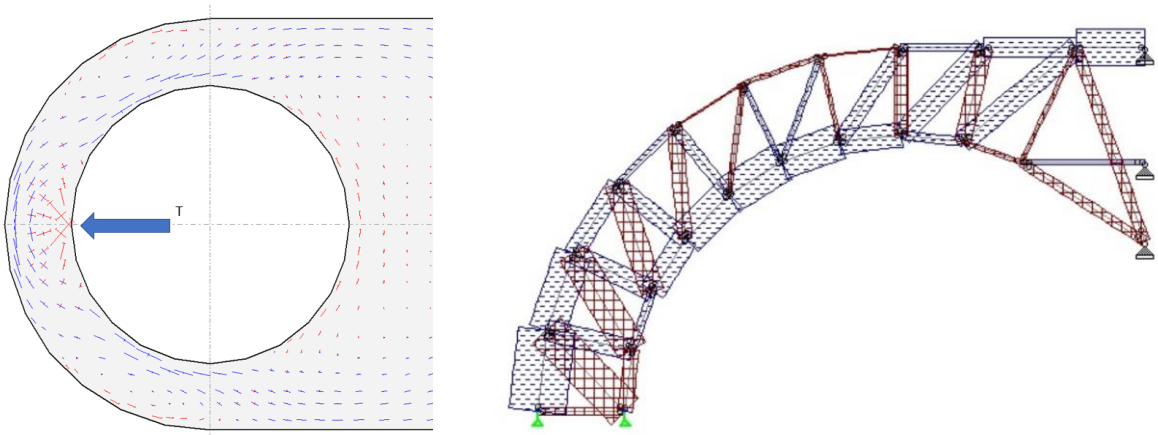

Figure 6-10 – Principal stresses in concrete of a 2D FE Model (left). Strut and tie model (right)

A 3D shell finite element model was elaborated in order to check the goodness of the previous model and assumptions. The following model shows just an example of the maximum principal stresses in the structure.

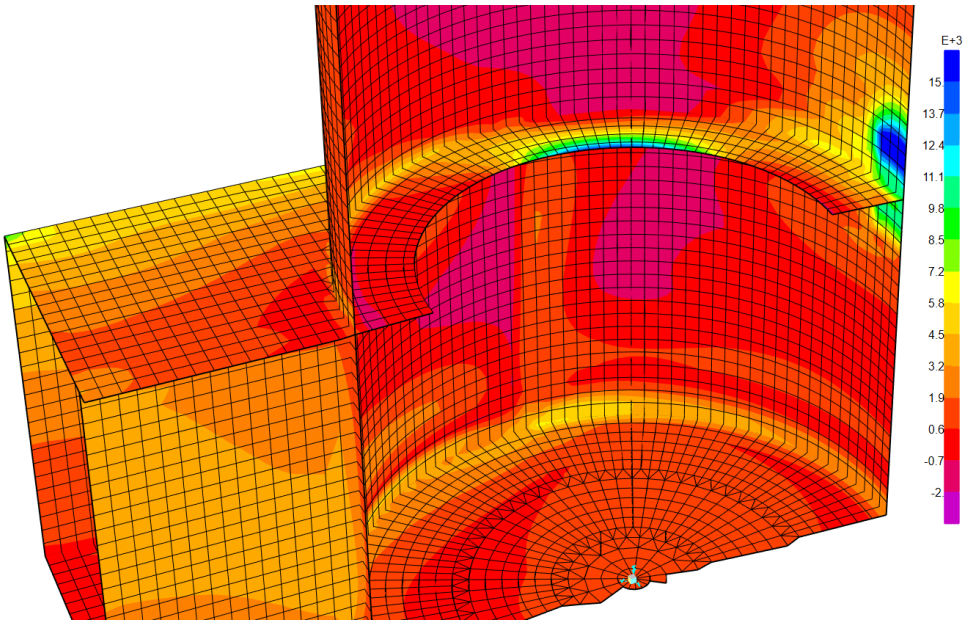

Figure 6-11 - Max. Principal stress (kN/m²)

7 Design Recommendations for Internal Structural Design of Concrete Floaters

7.1 Introduction

In this section the main structural design concepts for concrete offshore structures are presented. These design concepts and philosophy recommendations are obtained from the design process for the two concrete FOWTs, WindCrete and ActiveFloat. Also, a review and comparison of the main standards recommendations is presented. The topics that are covered in this section are post-tensioned concrete structures, water-tightness considerations, reinforcement, section analysis and particular structural sections.

7.2 Standard recommendations

7.2.1 General Order of Precedence

Conflicting requirements between codes and standards in offshore wind projects are resolved using an order of precedence. Requirements from a lower level of the hierarchy shall only apply when not in conflict with the requirements from a higher level of the hierarchy. An exemplary hierarchy for an offshore wind project is shown below [6]:

1. Authority laws, rules and regulations (national and regional)
2. Project specific requirements and specifications, e.g. defined in design basis
3. Owner's technical and professional requirements, e.g. for design, construction, T&I, O&M etc.
4. Codes and standards, e.g. as defined in design briefs
    a. Overruling status, e.g. by IEC
    b. Governing status, e.g. by DNV
    c. Mandatory status ("shall" regulations), e.g. by ISO or API
5. Other codes and standards
6. Industry best/recommended practices

The documents of items 2 & 3 typically refer to codes and standards in item 4. Depending on developer preferences, stricter requirements can be defined in item 2 & 3 than are required in item 4, such as for HSE aspects. Item 4 represents a set of standards agreed between the developer and the classification society usually defined in design briefs. Item 5 refers to codes and standards referenced in item 4 as well as additional standards that cover specific design aspects: Governing floating wind specific standard frameworks – i.e. IEC TS 61400-3-2, ABS 195, Bureau Veritas NI572 or DNV-ST-0119 – include references to national and international standards and rules, including but not limited to ACI, AISC, API, ASTM, AWS, BS, EEMUA, EN, IACS, IMO, ISO, ITTC, NACE, NORSOK and PTI. Other maritime class societies, such as the Japanese (ClassNK) or Italian (RINA) maritime class society, also have applicable standards and design guidelines for offshore wind turbines. The documents of item 6 provide guidance and recommendations on general principles and methods which shall be used in combination with the codes and standards of item 4 and 5.

7.2.2 Relevant Standards for Concrete Hull Structures

An exemplary hierarchy of standards and codes for structural design of concrete floating foundations is shown in Figure 7-1 with DNV-ST-0119 as exemplary governing technical standard for floating offshore wind turbines. Project level certification can be handled through DNV-SE-0422 while specific concrete related topics are addressed in EN 1992-1-1 supplemented by DNV-ST-C502 and IEC TS 61400-3-2.

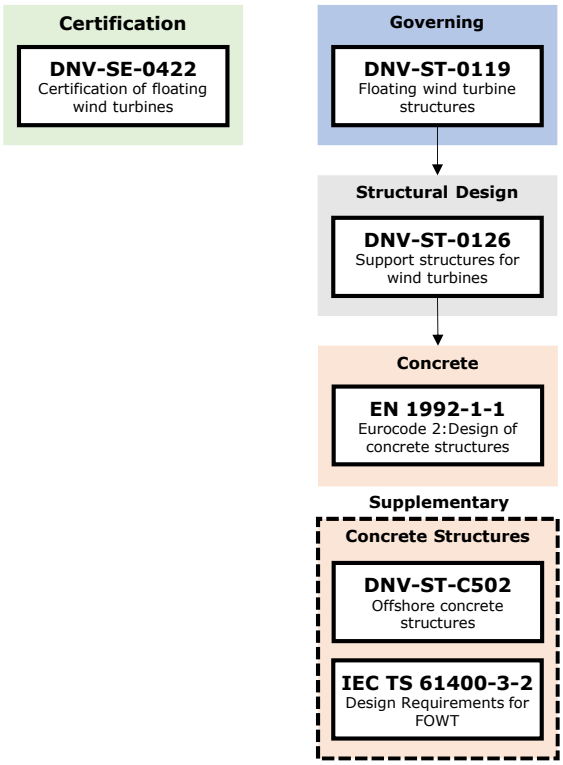

Figure 7-1: Exemplary standards applicable to structural design of FOWT concrete structures.

The governing floating wind standards are not fully consistent with respect to the design requirements for concrete floating foundations. For example, IEC TS 61400-3-2 does not cover concrete floating foundations, but refers to IEC 61400-3-1 which provides some guidance and references to ISO 19903 for fixed concrete structures. ABS 195 refers to ACI standards and gives additional design requirements and guidance on analysis and design of details for floating concrete structures. DNV-ST-0119 refers to DNV-ST-0126 in combination with DNV-ST-C502 or EN 1992-1-1 and states additional requirements.

Concrete structures for floating wind application are usually prestressed before they are taken into operation. Prestressing is applied by tendons or bolts, and the tendons may be pre-tensioned (before casting) or post-tensioned (after casting). A number of design standards from civil and offshore engineering relate to the design basis and methodology for prestressed concrete structures: EN 1992-1-1 of Eurocode 2, DNV-ST-0126, DNV-ST-C502 (also including requirements for fabrication and construction) or IEC 61400-6. Other relevant standards can apply like DIBt (German Institute for Civil Engineering) for German projects or “Model Code for Concrete Structures 2010” by fib (International Federation for Structural Concrete) – a pendant to EN 1992-1-1.

The inspection and maintenance requirements for prestressing systems depend on various parameters such as the type of system, the safety level of the structure etc. More generic information also regarding installation can be found in the ETA (European Technical Assessment) of the selected system. EN 1992-1-1 states a requirement that prestressed concrete structures shall show ductile behaviour in case of failure of a tendon, such that it is possible to replace the tendon without a sudden failure of the structure. The tendon could snap due to e.g. corrosion or local overstressing. Therefore, it is important that the anchorages should be regularly inspected to identify if there is any corrosion taking place. In some cases, the stress in the tendons can also be monitored to identify in real time if a tendon would gradually lose strength or would suddenly snap.

Modular precast concrete structures can be used for some floating foundation concepts and need to be connected with joints. Requirements for the detailed design of offshore concrete structures are included, for

example, in DNV-ST-C502, also with guidance on different connection types using grout (steel to steel, steel to concrete, concrete to concrete, and connecting precast concrete elements). From a risk perspective, every joint represents a discontinuity introducing a fragile element into the structure and adding complexity, risks and costs so that their number should be limited to the minimum. Permanently submerged floating offshore structures have different requirements than bottom fixed offshore or onshore structures. Watertightness and sufficient compression around the joint need to be ensured requiring sufficient post-tensioning. Inspection and maintenance plans require a valid strategy to monitor the joints. Quality of joints can be an issue during production as joints are produced on site and not in a controlled environment like a dedicated fabrication facility as possible for precast elements. Continuous slip forming is an alternative construction method for concrete structures to avoid potential issues arising from joints.

Corrosion is just as important for concrete structures as for steel but using different mitigation measures. In general, steel reinforcements can be protected with sufficient concrete cover and with limitations on crack widths in the design. However, a risk assessment is recommended to evaluate risks and benefits of providing additional measures for corrosion protection.

Recommendations for construction of concrete floating foundations are given, for example, in [7].

7.3 Design recommendations of floating concrete structures

Concrete structures are a type of offshore elements that have some particularities that makes them suitable for large span life offshore structures. This advantage within floating offshore wind turbines industry may allow to reduce the expected LCOE, but multiple considerations have to be applied. Large life spans over 50 years imply the design of structures with a far vision of the development and trends of the technology. Wind Turbines life span is about 25 years. Then, repowering the FOWT may imply the account of future needs of upcoming wind turbines, with larger power. Moreover, offshore is a very harsh environment, particularly for steel structures. Concrete structure also use steel components to improve the characteristics of mass concrete with very low tensile strength. The steel placed inside the concrete can be differentiate in passive and active steel reinforcement. The steel increases the capabilities of the concrete to resist bending moments while the concrete protects the steel by its alkaline nature producing a new structural material. The health of the reinforced concrete will depend in the health of either the steel and the concrete. Concrete cracking can induce the presence of water that can damage the steel reinforcement. Also, the carbonation of the concrete can induce the oxidation of the rebars due to the presence of chlorides in the sea water. Then, it is necessary to comply with high demanding requirements in order to ensure the reliability of the structure to support high load wind turbines for life span over 50 years.

7.3.1 Concrete characteristics recommendations

- **Concrete characteristics**

Concrete characteristics and properties are responsible of the durability and health of the concrete itself during the lifespan of the structure between 25 and 60 years. EN1992-1-1 Table 4.1 presents the exposure classes to be considered when defining concrete properties. The exposure classes considered herein are the corrosion induced by carbonation (XC) and by chlorides from sea water (XS). Different classes of exposure can be applied in different parts of the structure. For example the substructure base is permanently wet and submerged so XC1 and XS2 may apply, while splash zone in the MSL is defined as XC4 and XS3, and CX3 and XS1 may apply to tower sections.

The concrete used in offshore environment should present low pore intercommunication to prevent chlorides diffusion and to reduce the total material permeability. Then, it is important to ensure a good vibration and compaction during the construction process. Silica fume or other admixtures also may be added to increase the

concrete capabilities as the reduction of the permeability and the increase of the concrete strength due to its pozzolanic nature. The increase of the concrete strength may come from ULS requirements, but also there is a high probability that fatigue damage can drive to the concrete strength selection, in order to reduce the ratio between the mean concrete compression and the concrete strength.

Another very important parameter for the concrete durability is the required concrete cover. Concrete cover ensures the protection of the passive and active reinforcement, reducing the possibility of concrete carbonation at the reinforcement round zones. The cover ensures that the carbonation does not reaches the reinforcement by increasing the distance from the concrete surface. Also, chlorides from the environment have more difficulties to reach the reinforcement. The required nominal covers for the given classes of exposure are 45mm and 55mm for passive reinforcement steel and prestressing steel respectively. However, if ducts with diameters larger than 45 m are used, then the nominal prestressing steel cover needed is the minimum between the duct diameter and 80mm, with a cover addition of 10mm.

- **Concrete section analysis and design**

Post-tensioned concrete structures are types of structure that increase the bending strength by imposing an external compression through the tendons. The initial prestressing force imposes an initial stress distribution along the section depending the value and position of the equivalent axial force and the initial external loads such as weight. The prestressing provides a surplus compression range in order to reduce or avoid tensile stresses if tensile forces are applied. Thus, the initial prestressing force is design as a function of maximum allowable compression stresses for the service limit state, and the required section bending strength for the ultimate limit state. Concrete strength-stress relation is a very important ratio that will lead to final concrete strength choice. There are several concrete stress limitations when designing. First the maximum compressive stresses shall be less than $0.6f_{ck}$ and $0.45f_{ck}$for the characteristic extreme load and under permanent loads, respectively. Even the clear limitations of the maximum compression for the concrete design stated by the standards these limitations may not be enough in certain regions of the structure , in special if fatigue may be a limiting design factor. Second, concrete elements with a hydrostatic pressure difference between the external and internal parts shall be designed with a minimum permanent compression zone depending on the pressure difference. This requirement is applied for all the submerged part of the structure, and it is important to account for the hydrostatic pressure of the ballast that opposes to the sea hydrostatic pressure. Moreover, if the concrete element shall remain watertight to ensure floatability, according to the DNV standard, a 0.5MPa membrane compressive stress shall be guaranteed.

In offshore structures, cylindrical geometries are usually used. However, these types of geometry with ring sections are outside the scope of the typical sections described in the standards. Then, no valid equations are provided and detailed analysis are needed in order to ensure the stress distribution along the section accounting for the different types and positions of the reinforcement. This detailed analysis must be performed using fiber section analysis or high fidelity tools. This tools allow to assess the parabola-rectangle concrete stress-strain distribution, and account for the actual tension of the passive and active reinforcement. The use of simplified equations can lead to a miss prediction of the actual strength of the section. A comparison of the values obtained by a simplified model and a more detailed model are presented in the following.

Figure 7-2 shows the force distribution along the ring supposing the concrete cracked in it ULS due to tensile stress from bending moment considering an axial force applied (N_{ed}) plus the post-tensioning force. Equation (1) shows the maximum bending moment (M_{max}) for a ring section supposing that the pre-tension force (Po) is placed at the axis of the section. In both cases the contributions from inertia and stress variation of the tendons are neglected.

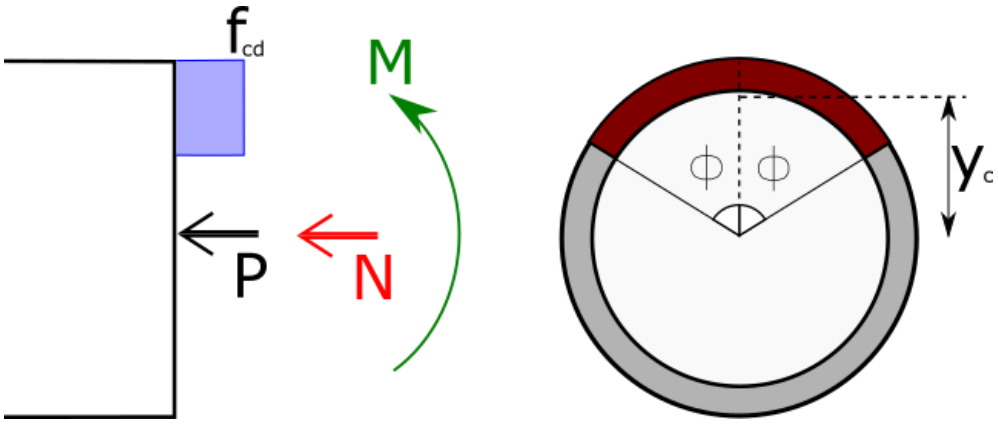

Figure 7-2: Simplified stress-strain section assessment

$$M_{max} = C \cdot y_C \tag{1}$$

Where C is the compression force at the section, y_c is the center of compressions, f_{cd} is the design concrete compression strength and ϕdefine the arch of the compression zone within the ring:

$$C = A_c f_{cd}$$

$$C = N_{ed} + P_0$$

$$A_c = 2\phi\left(R - \frac{t}{2}\right)t$$

$$y_c = \frac{\left(R - \frac{t}{2}\right)\sin(\phi)}{\phi}$$

Figure 7-3 shows the stress distribution for the same ring section but supposing the area of the post-tensioning tendons are equally distributed in a circumference with a radius equal to the middle radius of the ring. Then, the stress-strain state of the section can be solved by the newton method to get the curvature of the section by imposing axial force equilibrium and maximum compression stress at the concrete, as shown in Equation (2). Then, the maximum bending moment strength is assessed by Equation (3) as the integration of the stress by the lever arm from the middle of the section.

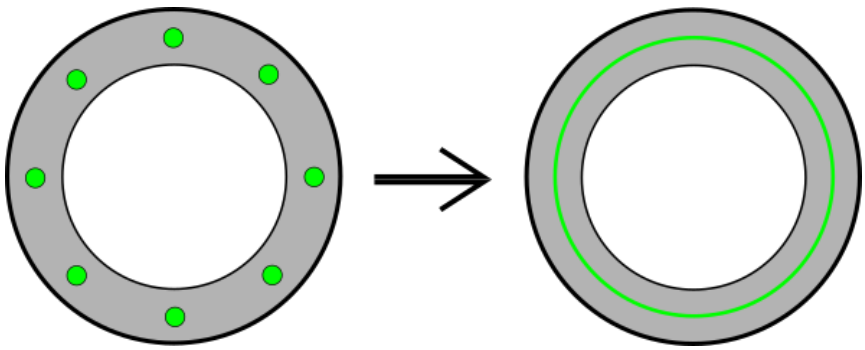

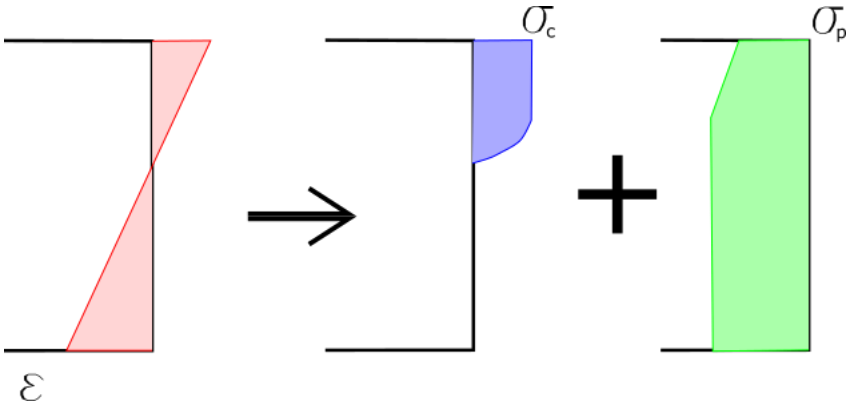

Figure 7-3: Ring section stress strain distribution

$$\mathbf{0} = \boldsymbol{Ne} + \int \boldsymbol{\sigma_p dA_p} - \int \boldsymbol{\sigma_c dA_c} \quad (2)$$

$$\boldsymbol{M_{max}} = \int \boldsymbol{\sigma_p z dA_p} + \int \boldsymbol{\sigma_c z dA_c} \quad (3)$$

The Figure 7-4 shows the actual strain, compression stress and posttensioning stress for the ring section in ULS condition. As can be seen, the compression stress follows the parabola-rectangle distribution. The post-tensioning stress shows that there is a reduction of the tension in the compression zone due to the imposed reduction of the strain in the compression zone.

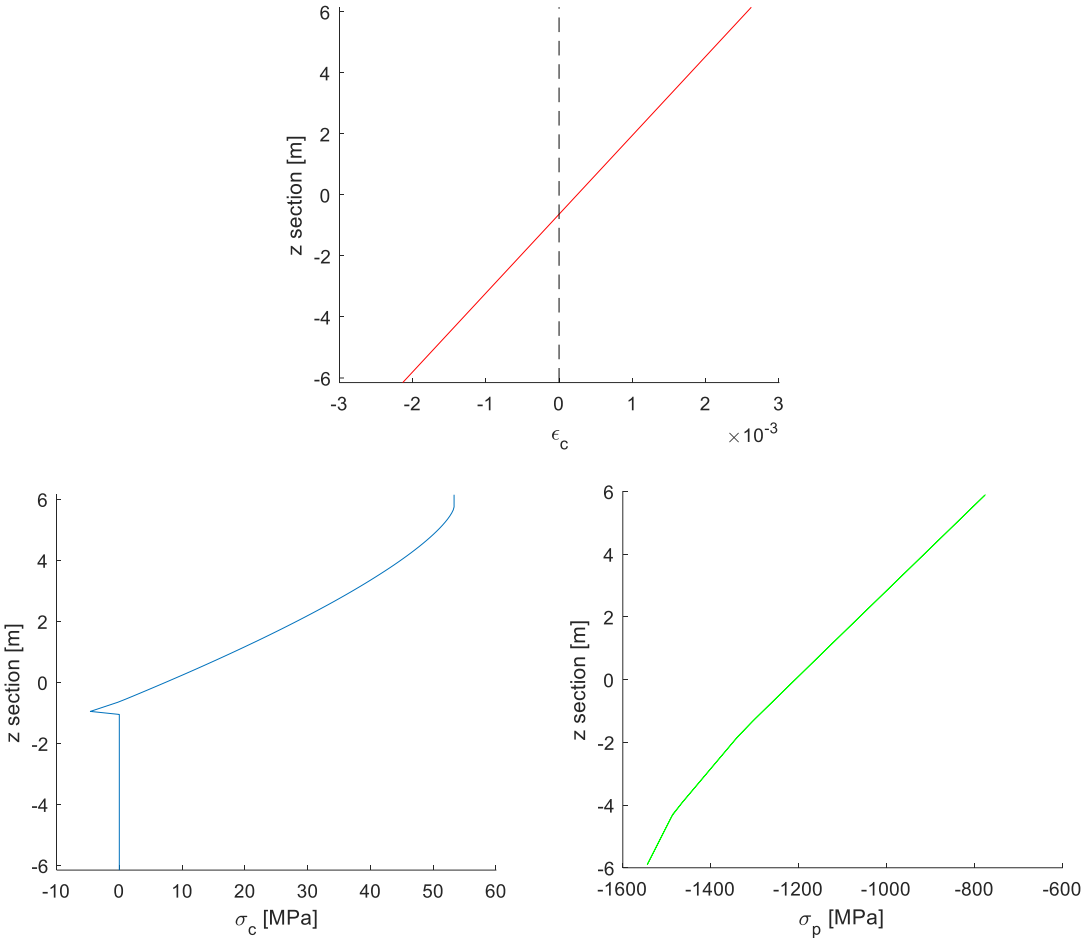

Figure 7-4: Strain (a), Compression concrete stress (b) and Posttensioning stress (c)

The results of a comparison of both methods in Table 7-1 show a reduction of the maximum resisted moment of 17% if the simplified method is used. The properties of the exemplary section and the results of the maximum resisted moment are shown in Table 7-1.

Table 7-1: ULS Moment Strength comparison

$\boldsymbol{R_e}$	$6.15\ m$
$\boldsymbol{t}$	$0.5\ m$
$\boldsymbol{f_{ck}}$	$80\ MPa$
$\boldsymbol{f_{pk}}$	$1674\ MPa$
$\boldsymbol{P}$	$3.665 \cdot 10^5\ kN$
$\boldsymbol{N}$	$5.192 \cdot 10^4\ kN$
	$\boldsymbol{M_u}$
Simplified	$1.67 \cdot 10^6\ kN \cdot m$
Integration method	$2.01 \cdot 10^6 kN \cdot m$

- **Reinforcement design**

Steel reinforcement is composed by both passive and active reinforcement. Passive reinforcement is designed mainly to ensure the minimum geometrical and mechanical reinforcement. Minimum geometrical passive reinforcement is given as a percentage of the concrete area. However, minimum mechanical reinforcement is designed to ensure the equivalent strength of the tensile zone of the concrete previous to cracking. On the other hand, section 7.3.2 (4) of the EC2 states that in prestressed members no minimum reinforce is required in sections where concrete is in compression for the characteristic combination of loads. Then, geometrical reinforcement should be applied. In such big structures, it is worth to differentiate two types of loads, the global section loads that acts over the whole section which simplify the platform as a vertical beam or column, and the local loads which are applied to the concrete wall associated with its shell behaviour. for submerged elements that shall remain watertight the minimum reinforcement should be at least twice the minimum recommended value of the applied standard.

The design of the active reinforcement has to ensure the reliability of the structure and provide the needed compression stress to the concrete to increase its bending strength performance. This strategy allows to delay the concrete cracking but taking into account the concrete compression stress limitations . As stated before, maximum concrete stress should be below $0.6f_{ck}$ and $0.45f_{ck}$for the characteristic extreme load and under permanent loads respectively. On the other side, the minimum compression stress at the concrete depends on the location and intact conditions of the designed element. For example submerged elements with external/internal hydrostatic pressure difference have to ensure a permanent compression zone according DNV-ST-0119 Section 7.5.1. Moreover, if the element shall remain watertight to ensure floatability the element shall be designed with a minimum compressive stress equal to 0.5MPa. However, these requirements do not apply to tower sections. It has to be stated that maximum compressions should be analyzed at start of construction, neglecting the time dependent post-tensioning losses, but minimum compressions should be analyzed at the end of the life span of the structure which will reduce the compressions provided by the tendons.

- **Fatigue considerations**

Concrete fatigue strength has a direct relation with the mean compressions, which can reduce drastically its fatigue behavior. Figure 7-5 shows the number of cycles that can be resisted by a concrete section as a function of the stress range and the mean compression. It is obvious that the increase of the mean compression reduces the total number of cycles that can be resisted for the concrete section. Fatigue analysis is a key point for the design verification of such structures. The FOWTs have a non-negligible motion range that influences the stress range of the structure which is related to the fatigue strength.

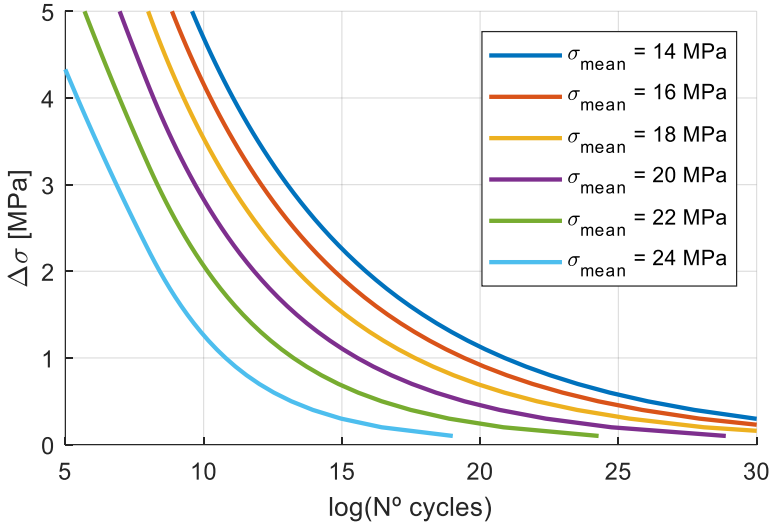

Figure 7-5: Concrete fatigue curves for 80 MPa strength.

- **Driven design Load Cases (ULS, SLS, FLS)**

Driving design load case for the structural design can vary depending on the type of FOWT, but also for the same FOWT different mooring configurations for example can result in different design driving load cases. Moreover, the design driving load cases may change depending on the structural element or the applied load analyzed. Then, it is very important to run the required simulations with a sufficient duration (e.g. 3h) to reduce uncertainties regarding stochastic process of the wind and wave in addition to performing multiple seed runs for each load case.

During the design process the DLCs found to be more important for the structural design are the DLC16 and DLC62. These design load cases account for wind and waves, different wind direction as well as yaw misalignment. This considerations may induce abnormal responses of the FOWT due to large torque moments on the turbine that can lead to larger internal loads. Also, emergency shut-down cases should be accurately studied and included in the fatigue assessment as they may occur many times during the life-span of the structure.

Other load cases that can be driving for design purposes are temporary load cases considering construction, transport or installation processes. In this stages, the structure can experience static conditions different to the operational conditions which may differ in terms of structural strength requirements. One example of this cases to be considered is the transport of a cylindrical element like a spar in horizontal position. For concrete structures, if a minimum compressive stress is needed, circumferential tendons may be used to avoid cracks on the structure. Also, storm conditions can induce large bending moments when parts of the platform emerge and behave as a cantilever beam.

- **Internal Load assessment and its application to structural models**

External load distributions are the source of motion accelerations and internal load distributions. However, many engineering tools used for floating wind turbines uses rigid body simplifications which imposes forces and moments to a unique point of the structure. Tower loads distribution can be assessed easily as wind turbines forces are applied at the top, and wind is applied as a distributed load. Moreover, due to the needs of accounting

the flexibility of the tower for the tower-turbine interaction, most models accounts for simplified FEM models that allow to assess the internal loads. However, substructures are usually assessed as rigid bodies and the hydrodynamic forces assessed by potential flow solutions, for which the integral of the surface pressures are applied to reference point. This leads to poor knowledge of the external force distribution on the substructure which is coupled with the dynamics of the FOWT. The assessment of the internal forces of the substructure can be done by the integration of the morison forces, for simplified models consisting of morison elements only, accounting for the acceleration of the nodes. This approach, allows to model the substructure as beams. However, this approach mismatch pressure distribution along the structure and does not allow to assess internal plate stresses. Moreover, these simplified morison models cannot account for diffraction effects even though simplifications such as MacCamy Fuchs theory can be applied [8]. On the other hand, FEM shell models can be used to predict internal plate forces. However, this is usually performed by applying external forces on the a post-process FEM model, where internal terms are difficult to apply and the platform at its undisturbed position is considered. The best approach is to perform a loads analysis in time domain with a fully coupled dynamic shell FEM model which comes however with a high computational cost.

7.3.2 WindCrete Spar platform with concrete tower particularities

- **Active tendon system**

WindCrete structural design is based on a set of longitudinal bonded tendons that starts at the tower top with increasing number of tendons towards the section at MSL. The increase of tendons is due to two reasons. First, as the tower cross section area increases a large number of tendons are required to provide the same initial compression stress. Second, the bending moment increases towards the section at MSL. Then, larger compression is required for the section to ensure the design requirement to avoid any tensile stresses in the concrete. From MSL downwards, the large increment of the substructure diameter allows to maintain a good pre-compression stress state in the cross section with a reduced number of tendons. Moreover, the internal loads in deeper sections are lower and the total number of longitudinal tendons can also be reduced.

- **Hemisphere considerations**

The hemispherical shape at the bottom of the spar is favourable in structural terms, distributing the hydrostatic pressures in a compression field around the base, while allowing the post-tensioning steel tendons continuously run through it. This continuity of the posttensioning tendons prevents point loads or discontinuities in the concrete stress field, that the use of dead end anchorages would introduce.

- **Yaw Bearing crown**

The yaw bearing crown is a special steel structural element that allow the connection between the structure and the yaw bearing. In order to ensure full load transmission between the crown and the tower, this is connected through the tendons anchor. A shown in Figure 7-6, the crown is composed by a round steel plate with an U-shaped cross section. This shape contributes to the stiffness of the crown, which is increased by the use of an upper plate that close the U-shaped one. By use of a flange at the top plate, the yaw bearing can be connected by bolts.

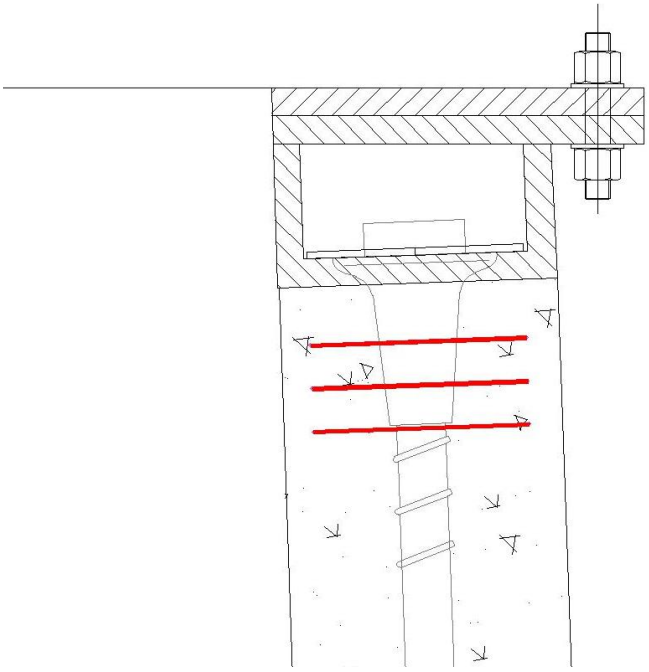

Figure 7-6: Crown sketch

- **Transition piece**

The transition piece is the tapered section between the tower and the cylindrical buoy. Its characteristics are defined in order to fulfil both hydrostatic and structural constraints. The hydrostatic constraints are defined by the required heave hydrostatic stiffness which directly depends on the waterplane to ensure the needed transition between the cylinder and the tower, thus, the top section of the transition piece. The structural constraints is driven by the optimization of the longitudinal post-tensioning tendons. The main purpose of the transition piece is to ensure continuity of the tendons between the tower and the cylinder buoy. Discontinuities of the curvature (e.g. between a cylindrical section and a conical section) reduce the total posttensioning force due to friction. Then, the transition piece has to ensure a smother change of the curvature from the tower apex angle to the cylindrical shape. Moreover, special care has to be applied at apex angle changes. As seen in Figure 7-7, the first angle change induces circumferential tension forces on the concrete, but in the lower section the resultant force introduces circumferential compression.

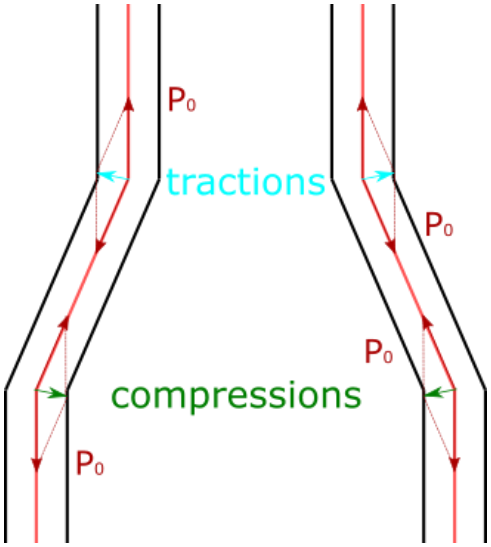

Figure 7-7: Transition piece with post-tensioning forces

7.3.3 ActiveFloat platform particularities

- **The steel tower is connected to the floater central column by a typical bolted flange connection.**

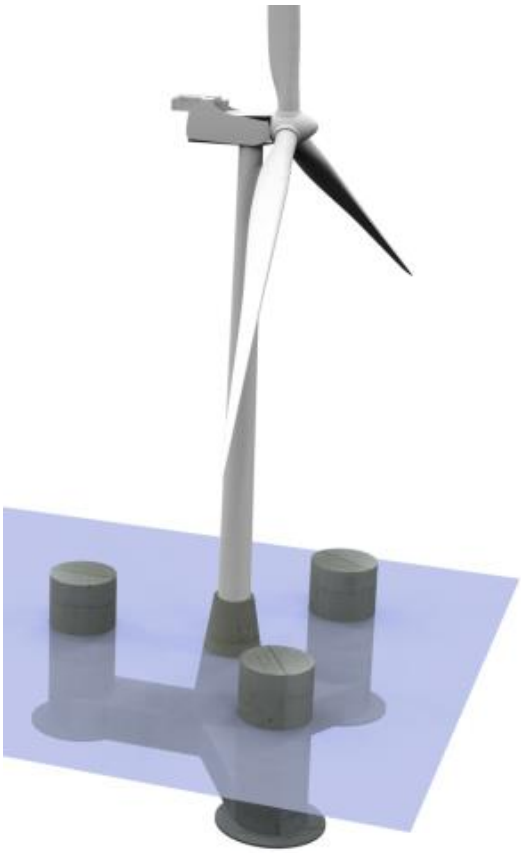

Figure 7-8 – General 3D view of Activefloat platform

- **Cone-shaped central column.**
    - It is a concrete transition piece between steel tower and pontoons.
    - It has an internal diaphragm at level of pontoons upper slab to adequately transfer the forces between the three pontoons.
- **Pontoons connecting central and external columns.**
    - Pontoons are fully ballasted with water.
    - Upper/lower slab prestressing tendons passing through central column.
- **External columns providing buoyancy and stability.**
    - They have cylindrical shape to better withstand the external seawater pressures.
    - They have an internal opened diaphragm inside at level of pontoons top face which receive the loads from the upper slab of the pontoons and is also used as the load path between the fairlead connection and the general structural system.
    - The concrete heave plates are located at the bottom as continuity of the pontoons lower slab.
- Fairleads connections.
    - They are located at level of internal diaphragm inside external columns so that the mooring forces are transferred in a robust structural element connected to the pontoons and limiting the structural contribution of the columns.

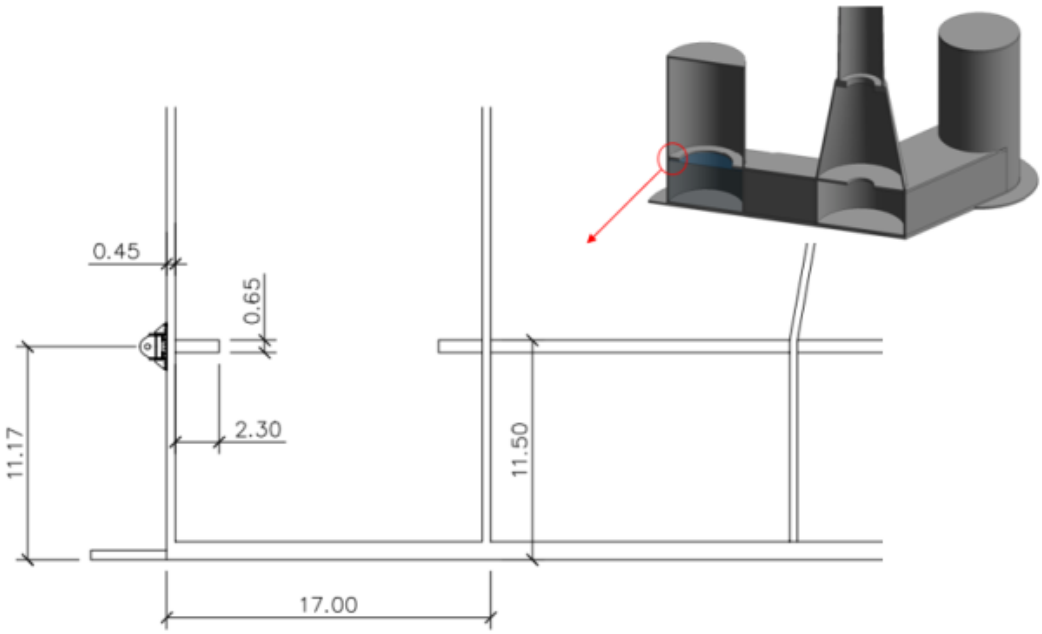

Figure 7-9 – Mooring anchoring point location (fairlead location)

8 Conclusions

This study presents the results of the studies performed within COREWIND project regarding the effects of the mooring system and dynamic cable design to the platform design, particularly the structural design and the mooring connections.

During the COREWIND project several mooring configurations have been studied and the implications on the platform response are assessed. First, a mooring system predesign was presented in D1.3 in order to allow the first simulations of the WindCrete and ActiveFloat models. These predesigns were set up for Active Float for Site A - West of Barra, Site B - Gran Canaria and Site C Morro Bay. In the case of WindCrete, the predesign mooring systems were set up for Site B - Gran Canaria and Site C - Morro Bay due to depth constrains. The optimized mooring systems for each design were presented in D2.2. These designs fulfil the ULS requirements but not the FLS requirements. Also, the effects of peak load reduction systems have been studied and were presented in D2.3, also including in its design the optimization process. Finally, the optimized mooring systems have been analysed through the experimental test campaign presented in D5.3. For the experimental setup, the Gran Canaria site was selected and a truncated mooring system was used to emulate the optimized mooring system design.

A global comparison of all the available data for each platform and site is difficult due to the limited cases which can be directly compared. In some cases there is a lack of data because there are different simulation setups and different DLCs and outputs. The available data presented in this document are the DLC 16 and DLC 61 for the predesign and optimized mooring system. The DLC 61 and DLC 61 for the peak load reduction system and the DLC 16 for the experimental results.

However, the general trend of the results can be used to derive the following main conclusions:

- The optimized mooring designs use to have lower line tensions in general compared with the predesign ones, which lead to a more economical design
- The optimized mooring designs have a positive effect on the platform structural design. The mooring system provide the Surge/Sway and Yaw stiffness required for the coupled FOWT-mooring system in the windcrete design. Then, a proper mooring system allows to reduce the tower base loads and nacelle accelerations , which at the same time implies a positive effect on the line tensions.
- The motions of the platform for the optimized ones have no common trend between WindCrete and ActiveFloat. WindCrete optimized mooring designs tend to reduce platform motions, whereas ActiveFloat ones implies a more compliant structure within the motion DOFs. Then, optimized mooring system differences rely on the initial behaviour of mooring system predesigns.
- The use of peak load reduction systems allows to reduce mooring line tension but the increase of costs do not allow its use from an economic point of view.

Also, a comprehensive study is presented from the structural point of view of the whole structural platform and the details of the mooring connection. This study covers a review of the main applicable standards, the philosophy of the design of the structure as well as some structural details of each platform.

The main conclusions arising from the mooring connection design review are the followings:

- A steel plate attached to the concrete wall by means of post-tensioning bars is a feasible and reliable solution for mooring connection designs

- Post-tensioning bars have to ensure enough compression between the plate and the concrete wall to balance the mooring tensions and provide the required shear friction force

- Design loads should be based on the capacity of the mooring or alternatively assessed based on the design loads obtained by the hydrodynamic simulations, including the ALS conditions.

- Anchor bolts and their post-tensioned forced should be designed so that there is no decompression under the base plate for the characteristic extreme load combination to avoid fatigue at the post-tensioning bars.

- The ultimate capacity of the anchor bolts shall be verified under the ULS and the ALS combinations allowing for plate decompressions. If decompression occurs, the tension in the post-tensioning bars have to be revised because it will be highly increased, as well as the reduction of the shear friction.

- A final fatigue assessment of the anchor bolts, reinforcement and concrete shall be carried out. In this particular, it is remarkable the beneficial effect of post-tensioning, as significantly reduces the stress range of the bars and on the contact.

- Water-tightness and cracking limits of the concrete shall be controlled.

The main conclusions arising from the overall structural review are the followings:

- Concrete characteristics have to suit the life span of the structure. This should be ensured use of the appropriate cement for the selected exposure class and the required concrete cover.

- The concrete strength is defined based on the required section strength to balance the external loads. Moreover, mean concrete stress to concrete strength ratio is related to fatigue in concrete sections.

- Active reinforcement design is limited by the maximum compressions stress allowed at the concrete sections, but on the other hand, it has to ensure the water-tightness by providing a sufficient compression stress margin for requested sections.

- Water-tightness is a strong factor related to concrete design. Sections that shall contribute to the damage stability of the platform shall be designed with minimum compressive stress of 0.5MPa. Then, special considerations have to be applied to ensure such stress state.

- Construction and installation processes may be driving the structural design for certain sections of the structure.

- FEM models as well as detailed section analysis are required for a proper structural design analysis.

- Local strengthening of the cylindrical walls of the two floaters is required in the sections where fairleads are connected because the forces on the fairleads are above 5 MN.

- Both floaters do not present any joints with interfaces between precasted concrete elements. They are monolithic substructures.

The main conclusions arising from the overall cable system review are the following:

- Results from dynamic cable modelling and testing shows the cable system loading on the platform has a negligible influence on moored platform motion.

- Cable system loading and exit angle requirements based on the cable system designed should be taken into account during the structural design of the cable entrance to platform.

- Design drivers for the cable system (such as reduction in costing) can impact the loading on this part for the structure on the platform, so a balance between structural design and cable system design is needed.

- In addition, care should be taken in platform's cable routing structure design to facilitate the smooth disconnection of the cabling system (for planned disconnection cases for maintenance of the platform, and for emergency disconnections) to prevent damage to the structure and minimise damage to the dynamic cabling.

- Unlike static windfarms (where cable systems are generally designed to fit in with predefined static turbine support structures), due to the inter-dependencies of the moored floating wind structure and the cabling system, the allowable motion for the moored platform structure needs to be considered with limits and cost impact on the cable system design, particularly in regards to target platform excursions relative to water depth.

9 References

[1] M. Y. Mahfouz, M. Salari, S. Hernández, F. Vigara, C. Molins, P. Trubat, H. Bredmose and A. Pegalajar-Jurado, "COREWIND, Deliverable D1.3, Public design and FAST models of the two 15MW floater-turbine concepts," 2020.

[2] M. Chemineau, F. C. V. Arramounet, P. Trubat, C. Molins, F. Vigara, G. d. Guglielmo, C. Cortés, M. Y. Mahfouz, Q. Pan, T. Bailey, M. Schilling, F. Borisade and X. Ren, "Corewind Deliverable 2.2: Design analysis and optimization of mooring & anchoring system for FOWT," 2022.

[3] L. Méchinaud, M. Chemineau, F. Castillo, M. Y. Mahfouz, Q. Pan, L. Willeke, H. Bredmose, O. Gözcü and N. Pollini, "COREWIND Deliverable 2.3: Exploration of innovations and breakthroughs of station keeping systems for FOWT," 2022.

[4] R. Guanche, M. Somoano, T. Battistella, J. Sarmiento, Á. Rodríguez-Luis, S. Fernández-Ruano, Á. Álvarez, D. Blanco, A. Facchinetti, A. Fontanella, S. D. Carlo, V. Arramounet, F. Castillo and P. Trubat, "COREWIND Deliverable 5.3: Integrated FOWT test report," 2022.

[5] S. Doole, F. Castillo, F. Borisade, J. I. Rapha and M. Somoano, "COREWIND D3.2 Analysis and Optimisation of dynamic cabling design for floating offshore wind farms," 2023.

[6] ORE Catapult, Ramboll, "FOW CoE: Application of Standards, Regulations, Project Certification & Classification – Risks and Opportunities," [Online]. Available: https://ore.catapult.org.uk/?orecatapultreports=fow-coeapplication-standardsregulationsproject-certification-classification-risks-opportunities. [Accessed 01 12 2022].

[7] F. Borisade, J. Bhat and D. Matha, "LIFES50+, Deliverable D5.5, Overall summary of the industrialisation process," 2019.

[8] P. Trubat, C. Molins, P. Hufnagel, D. Alarcón and A. Campos, "Application of morison equation in irregular wave trains with high frequency waves," in *Proceedings of the International Conference on Offshore Mechanics and Arctic Engineering - OMAE*, Madrid, 2018.

[9] F. Vigara, L. Cerdán, R. Durán, S. Muñoz, M. Lynch, S. Doole, C. Molins, P. Trubat and R. Guanche, "COREWIND, Deliverable D1.2 Design Basis," 2020.

[10] M. S. S. H. F. V. C. M. P. T. H. B. A. P.-J. Mohammad Youssef Mahfouz, "Public design and FAST models of the two 15MW floater-turbine concepts," COREWIND, 2020.